Effects of local nicotinic activation of the superior colliculus on saccades in monkeys

Masayuki Watanabe

Doctor of Science

Department of Physiological Sciences
School of Life Science
Graduate University for Advanced Studies

2004

Abstract

To examine the role of competitive and cooperative neural interactions within the intermediate layer of superior colliculus (SC), we elevated the basal SC neuronal activity by locally injecting a cholinergic agonist nicotine and analyzed its effects on saccade performance. After microinjection, spontaneous saccades were directed toward the movement field of neurons at the injection site (affected area). For visually guided saccades, reaction times were decreased when targets were presented close to the affected area. However, when visual targets were presented remote from the affected area, reaction times were not increased regardless of the rostro-caudal level of the injection sites. The endpoints of visually guided saccades were biased toward the affected area when targets were presented close to the affected area. After this endpoint effect diminished, the trajectories of visually guided saccades remained modestly curved toward the affected area. Compared to the effects on endpoints, the effects on reaction times were more localized to the targets close to the affected area. These results are consistent with a model that saccades are triggered by the activities of neurons within a restricted region and the endpoints and trajectories of the saccades are determined by the widespread population activity in the SC. However, because increased reaction times were not observed for saccades toward targets remote from the affected area, inhibitory interactions in the SC may not be strong enough to shape the spatial distribution of the low-frequency preparatory activities in the SC.

Introduction

Saccadic eye movements have been studied as probes for cognitive brain functions in psychophysical experiments in which manipulation of visual stimuli modulates saccade performance (Findlay and Walker 1999). It has been suggested that the saccade performance is well explained by the "dynamic interactions model" in which different motor commands compete for dominance in a winner-takes-all fashion, with excitatory interactions occurring between motor commands coding movements to closely clustered targets (Clark 1999; Findlay and Walker 1999; Godijn and Theeuwes 2002; Munoz and Fecteau 2002; Trappenberg et al. 2001). Several lines of evidence have suggested that the intermediate layer of superior colliculus (SC) is the field on which these interactions occur. The SC integrates input from several saccade-related areas and sends its output to the brainstem saccade generator circuits (Sparks and Hartwich-Young 1989). SC neurons are organized into a retinotopically coded motor map which specifies saccades toward the contralateral visual field. (Robinson 1972; Schiller and Stryker 1972). The SC has been suggested to have intrinsic circuits, which are known to have excitatory interactions between sites of close proximity (McIlwain 1982; Moschovakis et al. 1988; Pettit et al. 1999; Saito and Isa 2003) and inhibitory interactions between remote sites (Meredith and Ramoa 1998; Munoz and Istvan 1998). Furthermore, it has been shown that the activities of SC neurons correlate with the psychophysical phenomena (Dorris and Munoz 1995; Edelman and Keller 1998; Glimcher and Sparks 1993b; McPeek et al. 2003; Olivier et al. 1999; Port and Wurtz 2003; van Opstal and van Gisbergen 1990). Accordingly, the competition and cooperation within the SC motor map have been suggested to implement the dynamic interactions model. However, recent findings have cast doubts on the role of the SC in the competitive selection of different motor plans (McPeek et al. 2003; McPeek and Keller 2002; Ozen et al. 2004; Pare and Hanes 2003; Port and Wurtz 2003).

The manipulation of visual stimuli not only modifies the activities of SC neurons but also affects the activities of neurons in widely distributed regions in the brain. Therefore, to examine the direct

relationship between SC neural activity and behavior, artificial manipulation of SC neuronal activity is required (Stanford 2004). Electrical stimulation has been frequently used to activate neurons close to the stimulation site and the results are consistent with the predictions from the dynamic interactions model (Carello and Krauzlis 2003; Glimcher and Sparks 1993a; McPeek et al. 2003; Munoz and Wurtz 1993b). However, electrical currents stimulate not only the cell bodies of neurons directly but also antidromically and orthodromically activate fibers of passage as well. These artifacts could create an abnormal spatial distribution of activation states across various brain regions. Consequently, the resultant behavior could be caused by a mechanism different from that which operates naturally. The injection of bicuculline, a $GABA_A$ receptor antagonist, is another method which has been used to selectively activate SC neurons without affecting axons (Hikosaka and Wurtz 1983, 1985a; Munoz and Wurtz 1993b). However, it is difficult to quantitatively analyze the effects on purposive saccades since bicuculline injection in the caudal SC prevented monkeys from performing saccade tasks by frequently evoking fixation-breaking saccades toward the movement field of neurons at the injection site (affected area) in addition to inducing nystagmus (Hikosaka and Wurtz 1983, 1985a). Moreover, in the case of bicuculline injection, the resultant saccades would not reflect the change in neural activity in GABAergic systems.

It has been shown that the SC receives cholinergic projections from the pedunculopontine tegmental nucleus (Beninato and Spencer 1986; Graybiel 1978; Hall et al. 1989; Illing and Graybiel 1985) whose neurons exhibit activities related to performance of saccades (Kobayashi et al. 2002). We have clarified that cholinergic input excite the majority of neurons in the SC via activation of α4β2 type nicotinic receptors and M3 type muscarinic receptors and inhibit GABAergic synaptic transmission via activation of M1 and M3 muscarinic receptors on presynaptic terminals in rodent SC slices (Isa et al. 1998; Li et al. 2004; Sooksawate and Isa, unpublished observations). We previously reported that local microinjection of the cholinergic agonist nicotine into the monkey SC decreased the reaction time of saccades toward targets presented at the affected area (Aizawa et al. 1999). In

addition, we confirmed recovery from the nicotinic drug effect within the experimental session (Aizawa et al. 1999). Furthermore, it seems likely nicotinic agonism may directly elevate the activation of SC neurons while preserving the GABAergic inhibitory influence. For these reasons, it is likely that the microinjection of nicotine can be a powerful tool for modestly elevating the basal firing rate of SC neurons without stimulating fibers of passage. In this study, we used this method to alter the spatial distribution of neural activity across the SC and examined its effects on saccades.

Methods

Animals

All experimental procedures were performed in accordance with the National Institutes of Health Guidelines for the Care and Use of Laboratory Animals and approved by the Committee for Animal Experimentation at Okazaki National Research Institutes. The details of the surgical and data acquisition methods have been published previously (Aizawa et al. 1999; Kobayashi et al. 2002). Briefly, two male (monkey M and D) and one female (monkey H) Japanese monkeys (*Macaca fuscata*) weighing 8.5-12.5 kg were trained to perform a button press task for a liquid reward, sitting in a primate chair. After the training was completed, the monkeys were anesthetized with isoflurane and implanted with scleral search coils (Fuchs and Robinson 1966) and head holders. The monkeys were allowed to recover for >3 wks and trained to perform visually guided saccade tasks with their heads in a fixed position. Recording chambers tilted 38° posterior to the vertical axis were mounted on the skull by a separate surgical procedure and experiments were subsequently performed.

Behavioral procedures for visually guided saccades

Visual stimuli, behavioral tasks and data acquisition were administered via the Tempo/Win computing system (Reflective computing, St. Louis, MO). Horizontal and vertical eye positions were sampled at 1 kHz using the search coil technique (Fuchs and Robinson 1966). Visual stimuli were back-projected on a tangential screen at a distance of 28 cm from the eye. The onset and offset of the visual stimuli were synchronized with the projector's vertical refresh (non-interlaced refresh rate of 60 Hz).

Each trial was preceded by an inter-trial interval (varied randomly between 500 and 1500 ms) during which the screen was illuminated with diffuse white light to prevent dark adaptation. After the removal of the background light, a fixation point appeared at the center of the screen and the monkeys were required to direct their eyes toward the target and maintain fixation for 400-800 ms within a

fixation window (3-5 deg, square). The monkeys were trained to perform 3 different visually guided saccade tasks: step, overlap and gap tasks (the overlap and step tasks are sometimes referred to as the no-gap task in the following text). In the step task, a visual target appeared simultaneously with the offset of the fixation point. In the overlap task, the target appeared while the fixation point remained visible until the end of a trial. In the gap task, the fixation point was extinguished 200 ms prior to the appearance of the target. During the gap period, the monkeys were required to maintain fixation in total darkness. The target presentation was the go signal for visually guided saccades in all of the 3 tasks. The monkeys were required to immediately make a saccade to the target within 500 ms from the target onset and then to maintain fixation for 250-300 ms within a target window (3-10 deg depending on target eccentricity and the performance of the monkeys). The monkeys were given a liquid reward when they correctly performed each trial. Two different tasks were usually included in a block of trials with equal probabilities (the gap and overlap tasks or the gap and step tasks). Visual targets were arranged to be symmetrically (for example, the inset in Fig 3) or asymmetrically (for example, the inset in Fig 4) distributed around the fixation point. These arrangements of visual targets were successively implemented when multiple microinjections were made within single canula tract (see Injection procedures). For experiments in which the target arrangement was symmetric (7 and 5 experiments in monkey M and D, respectively), targets were presented at equally spaced 8 different directions in all but one experiment. When targets were asymmetrically arranged (15 and 7 experiments in monkey M and D, respectively), average numbers of targets in an experimental block were 6.7 and 4.7 in monkey M and D, respectively. Stimulus conditions were randomly presented with equal probability.

Since nicotine microinjection was expected to affect the saccade endpoint (as shown in Fig 6), the target window was not set during injection experiments. The monkeys were then allowed to make saccades anywhere and were rewarded if saccades were initiated after the onset of the targets. After misdirected saccades, the monkeys made corrective saccades toward the targets that still remained

visible until the end of the trial instead of staircase saccades toward the affected area (Fig 6). Data from trials in which the monkeys did not initiate saccades (monkey M: 2.0 and 3.5 % of trials before and after microinjection, respectively, monkey D: 1.5 and 1.4 % of trials before and after microinjection, respectively) or did not make corrective saccades toward the target following misdirected saccades (monkey M: 5.5 and 8.8 % of trials before and after microinjection, respectively, monkey D: 8.0 and 9.0 % of trials before and after microinjection, respectively) were excluded from off-line analysis of visually guided saccades (see Reaction times and endpoints).

Localization of SC

The location of the SC was identified by single unit recordings and magnetic resonance images. The extracellular activities of single neurons were recorded using tungsten microelectrodes (Frederick Haer, Bowdoinham, ME) with an impedance of 1-6 MΩ. Electrodes were positioned through stainless steel guide tubes (23 gauge) using a micromanipulator (MO-95, Narishige, Tokyo). The guide tubes were held in position with a delrin grid that was fixed to the recording cylinder (Crist et al. 1988). Activities of saccade-related neurons were recorded and their movement fields were qualitatively determined. The depth of the location of the neurons was confirmed in relation to the guide tubes. Functional identification of the SC was performed through electrical stimulation (< 20 μA, 500 Hz, 50 biphasic pulses of 200 μs width) delivered via the electrodes and evoked saccades were confirmed. The relationship between the evoked saccades and the position of electrodes on the grid was in agreement with the SC movement map reported previously (Robinson 1972). Stimulation sites where the amplitudes of evoked saccades were larger or smaller than 3 deg were referred to as being caudal or rostral regions, respectively.

Injection procedures

Nicotine (Sigma-RBI, St. Louis, MO) was dissolved in phosphate buffered saline (PBS; pH 7.4,

Gibco-BRL, Gaithersburg, MD) at concentrations of 10, 50 or 100 mM. To inject nicotine, a 30-gauge syringe needle with a microwire extending from the tip (Crist et al. 1988) was lowered into the SC to the same depth at which saccade-related neurons had been previously identified. Electrical stimulations were delivered via the microwire to confirm the location of the tip of the syringe needle. After control saccades were recorded, pressure injection of nicotine was made into the SC at a rate of 0.2 μℓ/min, over a period of 1-5 min. The injected volumes ranged from 0.2 to 1.0 μℓ. In some experiments, following on-line qualitative verification of the recovery from the nicotine microinjection, a second microinjection of nicotine was performed at different depth within the same canula tract (difference > 200 μm). As a control, an equivalent volume of vehicle (PBS) was injected into the same location where functional effects of nicotine microinjection on saccades had previously been observed on different days. A summary of the injections is shown in Table 1.

Data analysis

The onset and offset of saccades were identified by radial eye velocity criteria (threshold 30 deg/s) during off-line analysis. The center of the affected area was determined for each canula tract from saccades evoked by electrical stimulations delivered through the microwire of the syringe needle. In monkey H, only spontaneous saccades were analyzed. In monkeys M and D, spontaneous saccades, fixation-breaking saccades and visually guided saccades were analyzed.

Reaction times and endpoints

The reaction time of visually guided saccades was defined as the time to initiation of the saccade after target onset. Saccades whose reaction times were less than 80 ms were regarded as fixation-breaking saccades and separately analyzed from visually guided saccades. Setting this criterion to 70 ms did not affect the following results (data not shown). The saccade endpoint was quantified as the distance from the center of the affected area while its initial point was aligned to the

origin of the coordinate axes. A misdirected saccade was defined as a saccade, which did not terminate within an off-line window (a radius of 2.5 deg) placed at the center of a target. Misdirected saccades were included in the analysis of reaction times and endpoints of visually guided saccades if corrective saccades toward the target followed the misdirected saccades and then the eye position was confined within the off-line window during 80 ms period just after the offset of the target.

Curved trajectories

To quantify the curvature of visually guided saccades, the curvature index was defined as follows:

$$Curvature\ Index = sign\left(\sum \Delta S\right) \times \frac{\sqrt{\left|\sum \Delta S\right|}}{Amplitude}$$

where ΔS denotes an area enclosed by the trajectory and the straight line passing the initial point and endpoint of the saccade. The sign of the ΔS was positive if the segment of the trajectory in ΔS was curved toward the affected area and negative if the curvature was opposite. To exclude an erroneous effect of misdirected saccades on the estimation of the median of the indices, this analysis was restricted to saccades ending within the off-line target window. It is still possible, however, that the distribution of saccade endpoints obtained prior to microinjection was different from that after microinjection even if they were confined within the off-line target window. To eliminate the difference, an additional spatial window was defined based on the saccade endpoints before microinjection. The saccade endpoints before microinjection were applied to a principle component analysis and their standard deviations (SDs) were calculated for the first and second components. The additional window was set to cover 2 SDs from the mean of the endpoints. We did not analyze the data with saccade endpoints outside of this additional window. Furthermore, we excluded the most deviated saccade from data after microinjection when the median of the saccade endpoints before and after microinjection was significantly different (Mann-Whitney U-test $p < 0.05$). The statistical tests

and the exclusion of a saccade were then repeated until the tests did not reach statistical significance ($p > 0.05$). The curvature indices of the remaining saccades were normalized to the curvature indices before microinjection.

Statistical tests

Data obtained during the 15-minute period following microinjection ("injection" data) were statistically compared with data for the 15-minute period prior to the start of the microinjection ("baseline" data). The time window was extended by 1 minute if the number of trials included in this window was less than 10. The time periods during which nicotine affected saccades depended on several experimental conditions, such as the concentration and volume of nicotine and the location of the injection site (data not shown). Thus, in the summaries of results (Figs 2, 5, 8 and 10), the time-window for the "injection" data was shifted by 1-minute steps to maximize the absolute difference between the "baseline" and "injection" data (the extent of the differences was quantified by the probabilities derived from statistical tests). Saccade performance was rather variable in the behaving monkeys. To maintain the behavioral states of the monkeys, the shift of the time-window for the "injection" data was shifted by 1 minute and determined within 20 minutes following the start of microinjection so that the effect of microinjection became maximum. Mann-Whitney U-tests with Bonferroni correction were used to perform statistical comparisons between the "baseline" and "injection" data ($p = 0.05$ was divided by the number of the statistical tests repeated). Observation of recovery from the effects of nicotine began 20 minutes after the start of the microinjection. Recovery was confirmed by comparing 15-minutes of "recovery" data with the "injection" data (data not shown).

Task dependent effects on visually guided saccades

For the endpoints and trajectories of visually guided saccades, task dependent effects (gap task vs.

no-gap task) were examined for the "injection" data in which significant nicotinic effects (endpoint: a decrease in distances from the center of the affected area, trajectory: an increase in curvature indices, U-test $p < 0.05$ with Bonferroni correction) were observed in at least one of the tasks and differences between the tasks were not observed in the corresponding "baseline" data (U-test $p > 0.05$). Since saccade reaction times are shorter in the gap task than those in the no-gap task (Saslow 1967), a direct comparison between saccade reaction times after microinjection in the gap and no-gap task is not adequate. The effects of nicotine on saccade reaction times for each task were quantified using a receiver operating characteristic (ROC) analysis (Figs 11 and 12) (Green and Swets 1966). In the ROC analysis, histograms of reaction times before and after microinjection were compared. Each point in the ROC curve was the proportion of reaction times after microinjection exceeding an arbitrary criterion value as a function of that of reaction times before microinjection exceeding the same criterion. Entire curves are obtained by sweeping the criterion value through the range of the data. The integrated area beneath each ROC curve (ROC area) indicates the difference between the two distributions of the reaction times before and after microinjection. If the two distributions were not significantly different, the ROC area would be nearly equal to 0.5. On the other hand, if the distribution of reaction times after microinjection had smaller or larger values than that before microinjection, the ROC area would approach zero or one, respectively. In this analysis, the windows of time for both the "baseline" and "injection" data were extended to 30 minutes to obtain a sufficient number of saccades for each task (at least 20 trials). The analysis was restricted to the data in which a decrease in the reaction times of saccades was observed after microinjection in at least one of the tasks (Permutation test $p < 0.05$ with Bonferroni correction; Uka and DeAngelis 2004).

Task dependent effects on fixation-breaking saccades

Analyses of task dependent effects on fixation-breaking saccades were restricted to the saccades triggered within 80 ms from the target onset. The effects on the frequency of fixation-breaking

saccades were quantified for each task (gap or no-gap task) by subtracting the proportion of trials in which fixation-breaking saccades were generated before microinjection from that of trials after microinjection (Fig 14A, " Δ error rate"). The endpoints of fixation-breaking saccades after microinjection were also compared between the tasks (U-test $p < 0.05$ with Bonferroni correction).

Results

Thirty-three nicotine microinjections in 22 canula tracts were made at 5 superior colliculi in 3 monkeys (monkey M: 11 microinjections in each colliculi, monkey D: 9 and 3 microinjections in left and right colliculi, monkey H: 3 microinjections in left colliculus, Table 1). We first analyzed the effects of nicotine microinjection on spontaneous saccades recorded during the inter-trial intervals of the visually guided saccade paradigms; this allowed us to examine the excitatory effects of nicotine regardless of the arrangement of targets within the experimental blocks. The effects of nicotine microinjection on performance of visually guided saccades and occurrence of fixation-breaking saccades were then examined.

Spontaneous saccades

Figure 1 shows the distribution of the endpoints of spontaneous saccades whose initial points were aligned to the origin of the coordinate axes. Prior to microinjection of nicotine (Fig 1A), the endpoints of spontaneous saccades were evenly distributed. In contrast, saccades were frequently directed toward the affected area following nicotine microinjection (Fig 1B, 100 mM, 0.6 μℓ, experiment N15-1 compared to Fig 1A, U-test $p < 0.0005$). Saccades directed opposite to that of the affected area were also increased after nicotine microinjection (Fig 1B). These are mostly return saccades to the center of the screen following the spontaneous saccades toward the affected area. The endpoint bias toward the affected area diminished with time (Fig 1C compared to Fig 1B, U-test $p < 0.0005$).

Summary of effects on spontaneous saccades

Figure 2 summarizes the effects on saccade endpoints from experiments in which the “baseline” and “injection” data could be compared. The distances of saccade endpoints from the center of the affected area were consistently decreased by nicotine microinjection (Fig 2, monkey M: 11 out of 20

experiments, monkey D: 8 out of 12 experiments, monkey H: 2 out of 3 experiments, U-test $p < 0.05$ with Bonferroni correction, pooling all data, Wilcoxon test $p < 0.0005$), indicating that nicotine microinjection facilitates generation of spontaneous saccades toward the affected area. Remarkable effects were observed for the data points plotted at the lower left portion of the summary figure. These plots were derived from experiments in which nicotine microinjection was made at the rostral region, which caused repeated generation of small contraversive staircase saccades toward the affected area (data not shown). Thus, marked effects were observed when the distance between the affected area and intended endpoints of spontaneous saccades (mostly smaller than 20 deg, see Fig 2A) was short.

Reaction times of visually guided saccades

Injections into caudal regions

If there is mutual facilitation between proximal sites and mutual inhibition between remote sites on the SC map as suggested by the dynamic interactions model (Clark 1999; Findlay and Walker 1999; Godijn and Theeuwes 2002; Munoz and Fecteau 2002; Trappenberg et al. 2001), saccadic reaction times were expected to be decreased when targets were presented close to the affected area while reaction times would be increased when targets were presented at a distance remote to the affected area after nicotine microinjection. Figure 3 shows the results from the same experiment shown in Figure 1 in which targets were presented in 8 directions (N15-1). Consistent with the prediction, the reaction times of saccades toward a visual target close to the center of the affected area were markedly decreased after nicotine microinjection in both the gap and overlap tasks (Fig 3A, U-test $p < 0.0005$). However, the reaction times of saccades toward a remote visual target were not increased (Fig 3B, gap and overlap, U-test $p > 0.05$). The same results were observed for other remote targets (Fig 3C). It might be possible that the effect of nicotine at the injection site was not strong enough to drive the inhibitory interactions in the SC. However, fixation-breaking saccades were frequently evoked toward the affected area after microinjection of nicotine (Fig 13), suggesting that

neuronal activity at the injection site was sufficiently elevated via nicotine exposure.

Injections into rostral regions

We next examined the effects of nicotine microinjected into the rostral region of the SC on the reaction times of saccades passing beyond the affected area (N5-1, Fig 4). Neurons in this region have been shown to exhibit tonic activity during fixation in addition to phasic presaccadic bursting activity corresponding to the movement field of the neurons (Krauzlis et al. 1997, 2000; Krauzlis 2003; Munoz and Wurtz 1993a). Accordingly, nicotinic activation of neurons in this region was hypothesized to increase the reaction times of saccades toward visual targets with large eccentricities and expected to decrease those of saccades toward visual targets with small eccentricities. Saccades toward targets with the same eccentricity were pooled since they showed similar results. In agreement with the hypothesis, the reaction times of saccades toward the targets with small eccentricity were decreased after microinjection (Fig 4A, U-test $p < 0.0005$). However, the reaction times of saccades toward the targets with large eccentricity were not increased (Fig 4B, U-test $p > 0.05$). The effects on the saccadic reaction times clearly depended on the target eccentricities (Fig 4C). Fixation-breaking saccades were frequently evoked toward the affected area after nicotine microinjection in both tasks (data not shown), suggesting that neurons close to the injection site were highly activated. The data for the gap task were excluded from the current analysis since a sufficient number of visually guided saccades was not obtained due to frequent generation of fixation-breaking saccades immediately following the fixation point offset by microinjection at the rostral region (Fig 15B).

Summary of effects on reaction times

Figure 5 summarizes the effects of nicotine microinjection on the reaction times of visually guided saccades (monkey M: 121 targets in 18 experiments, monkey D: 73 targets in 12 experiments). These results are shown in the coordinates of the SC motor map (Ottes et al. 1986). The amplitude

and direction of each target were first normalized to 1 and 0 on the Cartesian coordinate, and the position of the corresponding affected area was also converted to maintain its relative position with the target. The normalized target and converted affected area were then plotted on the SC motor map. The scatter plots in Figure 5 were created by applying this method to all targets. Although data for the gap task and those for the no-gap (step or overlap) task were pooled, the data points were almost evenly distributed when the analysis was applied to the data from different tasks separately (data not shown). A decrease in saccadic reaction times was restricted to the data points (injection sites) near the normalized target point (Fig 5A, monkey M: 32 targets in 14 experiments, monkey D: 17 targets in 7 experiments, U-test $p < 0.05$ with Bonferroni correction). Only two data points from one experiment showed an increase in saccadic reaction times (Fig 5B, monkey D, U-test $p < 0.05$ with Bonferroni correction). No changes in saccadic reaction times were observed for the data points remote from the normalized target point (Fig 5C, monkey M: 89 targets in 17 experiments, monkey D: 54 targets in 12 experiments, U-test $p > 0.05$ with Bonferroni correction).

Endpoints of visually guided saccades

Injections into caudal regions

In addition to the effects on reaction times, the endpoints of visually guided saccades were affected by nicotine exposure. Figure 6 shows endpoint effects from the same experiment shown in Figures 1 and 3 (N15-1). The trajectories of saccades before and after microinjection toward 3 different targets are shown in Figures 6A and B, respectively. The endpoints of saccades for the target proximal to the affected area were biased toward the affected area (red lines in Fig 6A and B). The biased saccades were followed by the corrective saccades (Fig 6B). This effect gradually diminished with time (Fig 6C). In contrast, the endpoints of saccade toward the target remote from the affected area were not changed by the microinjection (black lines in Fig 6A and B). For the target presented between the above two targets, the endpoints of saccades for the target were also biased toward the

affected area (blue lines in Fig 6A and B). The duration of this effect, however, was much shorter than that for the target close to the affected area (Fig 6D compared to Fig 6C). The effects on the saccade endpoints were restricted to the targets close to the affected area (Fig 6E).

Injections into rostral regions

Figure 7 shows the effects of nicotine microinjection into the rostral region of the SC on the amplitude of saccades from the same experiment shown in Figure 4 (N5-1). The amplitude of saccades toward the targets of intermediate eccentricity (15 deg) became shorter, followed by gradually diminished effects with time (Fig 7A). The amplitudes of saccades toward visual targets with large eccentricity (25 deg) also became shorter (Fig 7B). However, the effect was short lasting (Fig 7B) in contrast to the effect on the saccades to the targets with intermediate eccentricity (Fig 7A). A significant effect on amplitude was found for saccades toward the above targets (Fig 7C).

Summary of effects on endpoints

The effects of nicotine microinjection on the endpoints of visually guided saccades are summarized in Figure 8, using the same format as Figure 5 (monkey M: 121 targets in 18 experiments, monkey D: 73 targets in 12 experiments). A bias of saccade endpoints toward the affected area was mainly observed for the data points near the normalized target point (Fig 8A, monkey M: 22 targets in 13 experiments, monkey D: 17 targets in 7 experiments, U-test $p < 0.05$ with Bonferroni correction). Although a bias of saccade endpoints away from the affected area was also observed, the number of data points was small (Fig 8B, monkey M: 5 targets in 4 experiments, monkey D: 2 targets in 2 experiments, U-test $p < 0.05$ with Bonferroni correction). The endpoints of saccades toward targets remote from the affected area were not changed (Fig 8C, monkey M: 94 targets in 18 experiments, monkey D: 54 targets in 12 experiments, U-test $p > 0.05$ with Bonferroni correction).

Relationship between effects on reaction times and endpoints

As shown in Figures 3 and 6 and Figures 4 and 7, the effects on the reaction times of visually guided saccades were more localized than those on the endpoints of saccades. To compare the extent of nicotinic effects on the reaction times and endpoints of saccades, we calculated average distances between the affected area and targets toward which saccades were significantly modified (decreased reaction times or biased endpoints toward the affected area) for each experiment in which both reaction time and endpoint effects were observed. The average distances for reaction time data was significantly smaller than those for endpoint data (12 and 5 experiments in monkey M and D, respectively, pooling all data, Wilcoxon test $p < 0.0005$), indicating that nicotinic effects on the reaction times of saccades are more localized than those on the endpoints of saccades.

Curved trajectories of visually guided saccades

Recent studies using recordings of neural activity and electrical stimulation have suggested that the activities of SC neurons can affect saccade trajectories (McPeek et al. 2003; Port and Wurtz 2003). However, as previously mentioned in the introduction, these results should be revisited using microinjection of pharmacological agents, such as nicotine. Figure 9 shows an example of the effect of nicotine on saccade trajectories (N22-1). In this experiment, the endpoints of some saccades were biased toward the affected area (data not shown). Such biased saccades were excluded from analysis (see Methods) and the records shown in Figure 9 were restricted to saccades correctly directed toward the target. The post-microinjection trajectories ("injection", red line) were modestly curved toward the affected area compared to those recorded prior to microinjection ("baseline", blue line) (Fig 9A). To quantify these trajectories, the curvature index was calculated for each saccade (see Methods). A positive value of the index indicates a curved trajectory toward the affected area while a negative value indicates curvature away from the affected area. The time-course of changes in the normalized indices (Fig 9B, see Methods) shows that an increase in the indices emerged immediately following

nicotine microinjection and persisted for approximately 15 minutes (U-test $p < 0.0005$).

In the experiment shown in Figure 6 (N15-1), curved saccades were also generated. For the saccades toward the target 90° remote from the affected area (blue lines in Fig 6A and B), the bias of the saccade endpoints disappeared immediately following microinjection of nicotine (Fig 6D). However, the trajectories of the target-directed saccades remained modestly curved toward the affected area (U-test $p < 0.0005$).

Summary of effects on trajectories

The effects of nicotine microinjection on the trajectories of visually guided saccades are summarized in Figure 10 (monkey M: 117 targets in 18 experiments, monkey D: 72 targets in 12 experiments). Curved trajectories toward the affected area were more frequently observed for the data points near the normalized target point (Fig 10A, monkey M: 14 targets in 9 experiments, monkey D: 13 targets in 8 experiments, U-test $p < 0.05$ with Bonferroni correction). Although we observed trajectories curved away from the affected areas, the number of data points was small (Fig 10B, 3 targets in 3 experiments in each monkey, U-test $p < 0.05$ with Bonferroni correction).

Task dependent effects on visually guided saccades

In most experiments, the gap and no-gap tasks were randomly mixed in an experimental block. The effects of nicotine microinjection on visually guided saccades were clearly observed in both tasks across several saccade parameters (Figs 3, 6 and 9). It has been shown that the low-frequency preparatory activities of SC neurons are different between the tasks (Dorris and Munoz 1995; Dorris et al. 1997). Accordingly, it is possible that the effects of nicotine microinjection on visually guided saccades are task dependent. We did find task dependent effects on saccade reaction times but not on the saccade endpoints (monkey M, all of 4 targets in 4 experiments, monkey D, 9 targets in 5 experiments out of 11 targets in 6 experiments, U-test $p > 0.05$ with Bonferroni correction) and

trajectories (monkey M, all of 2 targets in 2 experiments, monkey D, 3 targets in 3 experiments out of 5 targets in 3 experiments, U-test $p > 0.05$ with Bonferroni correction). Figure 11 shows another example of the effects of nicotine microinjection on the reaction times of visually guided saccades (N19-1). In this experiment, the effect on saccadic reaction times lasted over 1 hour in the gap task while saccadic reaction times for the step task (Fig 11A) and the effects on spontaneous saccades during the task block (data not shown) were already recovered. ROC analysis was applied to quantify the difference between the pre- and post microinjection reaction times for each task (Fig 11B). When the time-windows for the data ranged from 0 to 30 min after the start of the microinjection, the ROC areas for the gap (black dotted line) and step (no-gap) tasks (black continuous line) were 0.12 and 0.17, respectively (Fig 11B). The difference in the effects between the tasks was more evident when the time-windows for the analysis were set to range from 30 to 60 min after the start of the microinjection: the ROC areas were 0.25 and 0.40 for the gap (red dotted line) and step (no-gap) tasks (red continuous line), respectively (Fig 11B). Figure 12 summarizes the results from the analysis in which the time-windows for "injection" data were set to range from 0 to 30 min after the start of microinjection. Most data points were above the equality line (monkey M: 12 targets in 7 experiments, monkey D: 10 targets in 4 experiments, pooling all data, Wilcoxon test $p < 0.005$), indicating that the effects for the gap task were more evident than those for the no-gap tasks. The same result was observed regardless of the position of the time-window for the "injection" data (data not shown).

Task dependent effects on fixation-breaking saccades

The frequency of fixation-breaking saccades was increased following microinjection of nicotine. Figure 13 shows the results from the same experiment shown in Figures 1, 3 and 6 (N15-1). Compared to the "baseline" data (Fig 13A), the number of fixation-breaking saccades during the gap task was markedly increased after microinjection, and these saccades were directed toward the affected area (Fig 13B and C). However, in the case of the overlap task, the fixation-breaking

saccades were not so frequently generated even after microinjection, and their endpoints were not always associated with the affected area (Fig 13B and C). Figure 14 summarizes the effects of nicotine microinjection on fixation-breaking saccades (19 and 10 experiments in monkey M and D, respectively). The "Δ error rate" indicates the differences of the proportions of pre- and post-microinjection trials in which fixation-breaking saccades were generated. A positive value of the Δ error rate indicates more frequent generation of fixation-breaking saccades following nicotine microinjection. The distribution of the Δ error rate was biased toward positive values in the gap task (sign test $p = 0.06$ in monkey M, $p < 0.05$ in monkey D), indicating that nicotine microinjection facilitates generation of fixation-breaking saccades in the gap task. Although the frequency of fixation-breaking saccades was also modestly increased in the no-gap task, the changes did not reach statistical significance ($p > 0.3$ in both monkeys). For experiments in which the frequency of fixation-breaking saccades was increased after microinjection in at least one of the tasks (15 and 9 experiments in monkey M and D, respectively), the rates of increases were higher in the gap task than those in the no-gap task (Wilcoxon test $p < 0.05$ in both monkeys), indicating that facilitation of fixation-breaking saccades was more evident in the gap task than those in the no-gap task. The endpoints of fixation-breaking saccades after microinjection in the gap task were compared to those in the no-gap task (Fig 14B, 7 experiments in both monkeys). The distance of saccade endpoints from the center of the affected area in the gap task was smaller than those in the no-gap task (2 and 5 experiments in monkey M and D, respectively, U-test $p < 0.05$ with Bonferroni correction, pooling all data, Wilcoxon test $p < 0.005$), indicating that fixation-breaking saccades in the gap task were more closely directed toward the affected area than those in the no-gap task.

Reaction times of fixation-breaking saccades from fixation point offset

Fixation-breaking saccades were frequently generated during the gap period of the gap task in addition to the 80 ms period following the target onset. Figure 15 shows the reaction times of

fixation-breaking saccades from the fixation point offset in the gap task when microinjection was made at the caudal (Fig 15A, N15-1, the same experiment shown in Figs 1, 3, 6 and 13) or rostral (Fig 15B, N1-1, amplitude of affected area < 3 deg) region. The frequencies of fixation-breaking saccades were markedly increased following nicotine microinjection in both experiments (Fig 15A and B). However, a transient decrease in the reaction times of fixation-breaking saccades from the fixation point offset was observed only when microinjection was made at the rostral region (Fig 15B, U-test $p < 0.0005$). Consistent results were observed in other experiments in which the "baseline" and "injection" data could be compared (microinjection at rostral region: 3 experiments in monkey M, U-test $p < 0.05$ with Bonferroni correction, microinjection at caudal region: 6 and 11 experiments in monkey M and D, respectively, U-test $p > 0.05$ with Bonferroni correction).

Vehicle injections

Vehicle microinjections of PBS were performed into the caudal SC, at the same location where significant effects of nicotine on saccades had been observed on previous days. For spontaneous saccades, the distances of saccade endpoints from the center of the affected area were not consistently changed, although the changes often reached statistical significance (increase: 1 experiment in monkey M, decrease: 2 experiments in monkey M, U-test $p < 0.05$ with Bonferroni correction). Figure 16 shows the reaction times of visually guided saccades from one of the experiments in which a significant decrease in the distances of the endpoints of spontaneous saccades from the center of the affected area was observed (P2-1). The reaction times of saccades toward a target close to the center of the affected area were unchanged after PBS microinjection (Fig 16A, U-test $p > 0.05$). The saccade reaction times were not changed by PBS microinjection regardless of the location of the targets (Fig 16B, U-test $p > 0.05$). Therefore, the significant change in the endpoints of spontaneous saccades was not supposed to reflect the non-specific actions of vehicle microinjection.

Discussion

We have shown that microinjection of nicotine into the SC of monkeys altered a number of saccade-related parameters. Although the effects of nicotine on the reaction times of saccades persisted in some experiments (Fig 11), we verified recovery in other parameters from drug exposure within each experimental session, eliminating the possibility that effects were due to non-specific damage at the injection site. These results are consistent with our original hypothesis that nicotine enhances the activity of saccade-related SC neurons. The modest excitatory effects by nicotine gave us an opportunity to study the relationship between the spatial distribution of SC neuronal activity and saccade performance. We first discuss the limitation of nicotine microinjection, and then temporal modulation of the activity of neurons at the injection sites and the relationship between the spatial distribution of neuronal activation states across the SC and the resultant saccades.

Limitation of nicotine microinjection

The excitatory effects of nicotine microinjection observed in this study are consistent with the previous report that application of acetylcholine agonists directly depolarized the postsynaptic membrane potential of SC neurons mainly via α4β2 nicotinic receptors in a rat slice preparation (Isa et al. 1998; Sooksawate and Isa, unpublished observations). As to the action of nicotine on the SC local circuits, we have found that not only excitatory neurons but also GABAergic inhibitory neurons are excited by nicotinic receptor activation (Sooksawate and Isa, unpublished observations). However, we did not observe any phenomena that are explained by enhanced inhibitory effects on saccade-related SC neurons. Therefore, it seems likely that the net effect of nicotine on the activities of neurons at the injection site is excitatory. Secondly, it has previously been shown that the regions where immunoreactivity of choline acetyltransferase is high are patchy and distributed more frequently in the caudal region than the rostral region (Graybiel 1978; Ma et al. 1991). Accordingly, the effects of nicotine microinjection on saccades might depend on the location of the injection site

relative to the "patch" of cholinergic fibers as well as the dose of nicotine. The answer to this question should wait for the detailed analysis of distribution of nicotinic acetylcholine receptors and patches of cholinergic fibers in the SC. However, we observed fairly pronounced excitatory effects of nicotine even when microinjection was made at the rostral region (Figs 4, 7 and 15B). Although the detailed mechanism of nicotinic activation of SC neurons should be clarified in the future, we suggest that nicotine microinjection is a useful tool for locally activating SC neurons.

Modulation of neuronal activity at injection sites

In previous studies in behaving monkeys (Hikosaka and Wurtz 1983, 1985a), bicuculline was used to elevate neuronal excitation within the SC. Bicuculline blocks $GABA_A$ receptors and disinhibits neurons at the injection site, leading to fixation-breaking saccades toward the affected area and finally inducing nystagmus. These monkeys were unable to inhibit the generation of these eye movements in any way because the fixation system could not affect neural activity at the injection site. Consequently, bicuculline injection prevented the monkeys from performing saccade tasks. Moreover, in the case of bicuculline injection, it may not be possible to observe the effects directly caused by the alteration of the GABAergic systems. In contrast, GABAergic inhibition seems to be intact following nicotine exposure, allowing the monkeys to perform saccade tasks. The results shown in Figures 13 and 14 are consistent with this notion due to the observation that after nicotine microinjection, fixation-breaking saccades directed toward the affected area were more frequently generated in the gap task than the no-gap task. During the gap period of the gap task, low-frequency preparatory activities of SC neurons are increased (Dorris and Munoz 1995; Dorris et al. 1997), which has been explained by decreased inhibition from the fixation system (Dorris and Munoz 1995; Dorris et al. 1997; Gore et al. 2002). If the activities of neurons at the injection site were under control of the fixation system as described above, such disinhibition would facilitate the effects of nicotine on the neural activation and thus cause more frequent generation of the fixation-breaking saccades toward

the affected area during the gap task. Task dependent effects of nicotine on the reaction times of visually guided saccades (Figs 11 and 12) also support the above discussion. Tonic elevation of the basal firing rate of SC neurons may contribute to a decrease in the saccadic reaction times in the gap and no-gap tasks. Moreover, judging from the stronger effects in the gap task (Figs 11 and 12), it is likely that the rate of elevation of the preparatory activities after the offset of the fixation point is increased after nicotine microinjection. Based on these considerations, we suggest that nicotine microinjection increased the rate of change in the activities of neurons at the injection site in addition to elevating the baseline activity.

Spatial distribution of activities for generation of saccades

The reaction times of saccades toward the targets close to the affected area were decreased immediately following nicotine exposure (Figs 3, 4 and 5). The preparatory activities of SC neurons have been shown to correlate with saccadic reaction times (Dorris and Munoz 1998; Dorris et al. 1997; Everling et al. 1999; Sparks et al. 2000). Thus, it is likely that nicotine enhanced the preparatory activation of neurons at the injection site and facilitated initiation of their presaccadic bursts. The endpoints of saccades toward the targets close to the affected area were biased to the affected area (Figs 6, 7 and 8), suggesting that the center of gravity of activities would be shifted toward the injection site (Badler and Keller 2002; Edelman and Keller 1998; Glimcher and Sparks 1993; van Opstal and van Gisbergen 1990). Compared to the effects on the endpoints, the effects on the reaction times were more localized to the targets close to the affected area (Figs 3 and 6, Figs 4 and 7, and Figs 5 and 8). This is in agreement with the assumptions of the SC model (Clark 1999; Findlay and Walker 1999; Godijn and Theeuwes 2002; Munoz and Fecteau 2002; Trappenberg et al. 2001) that saccades were triggered when the activities of neurons within a restricted region reach a constant threshold (Pare 2003) while the endpoints of the saccades were determined by the widespread activities across the SC (Lee et al. 1988; Robinson 1972). Our results do not exclude other

possible mechanisms. For instance, the threshold for triggering saccades might be changed after nicotinic activation if the firing rates of neurons within the local region of the SC are not so strictly related to the initiation of saccades (Liston and Krauzlis 2003). Simultaneous recordings of neural activity during nicotine exposure are required to establish whether the assumptions of the SC model hold true even after excitatory perturbation is directly applied to the SC.

Curved trajectories of saccades

It has recently been shown that the trajectories of target-directed saccades can be curved by presentation of distractors (Arai et al. 2004; Doyle and Walker 2001; Doyle and Walker 2002; McPeek et al. 2003; McPeek and Keller 2001; Port and Wurtz 2003). When curved saccades are generated, the spatial distribution of activities in the SC motor map is dynamically altered (McPeek et al. 2003; Port and Wurtz 2003), suggesting that the excitatory state of SC neurons can affect saccade trajectories. However, it is still possible that the curvature could be explained by input from saccade-related areas other than the SC, such as the frontal eye field (FEF), to the brainstem saccade generator circuits bypassing the SC (Quaia et al. 1998). A previous study showed that activation of SC neurons by electrical stimulation could bend saccade trajectories toward the movement field of neurons at the stimulation site (McPeek et al. 2003). However, electrical stimulation would create an abnormal spatial distribution of neuronal activation states due to its effects on fibers of passage. In current experiments, we used nicotine microinjection to locally activate SC neurons without stimulating axons. After nicotine microinjection, the saccade trajectories were slightly curved toward the affected area even after the endpoint effects of the saccades were diminished (Figs 6, 9 and 10). The modest effects on saccade trajectories might involve underestimation of the nicotine effects since we excluded some curved saccades from analysis if the saccade endpoints were biased toward the affected area (for example, upward saccades in Fig 6B, see Methods). The curved saccades caused by nicotinic activation support the view that activation of SC neurons can affect the trajectories of

saccades. As previously suggested, it is possible that neurons at the injection site receive natural synaptic drive during the curved saccades. Accordingly, dynamic changes in the spatial distribution of neural activation seem to be generated after nicotine exposure as in the cases of curved saccades induced by the presentation of distractors (McPeek et al. 2003; Port and Wurtz 2003).

Role of rostral SC in generation of saccades

The tonic activities of rostral SC neurons during active fixation have been suggested to be involved in maintenance of fixation (Gandhi and Keller 1997; Munoz and Wurtz 1993a). At the same time, the neurons also show phasic activities before small contraversive saccades, suggesting that they contribute to triggering small saccades (Krauzlis et al. 1997, 2000; Krauzlis 2003; Munoz and Wurtz 1993a). Nicotine microinjection made at the rostral SC facilitated small contraversive fixation-breaking saccades (Fig 15B). Furthermore, a transient decrease in the reaction times of fixation-breaking saccades from the fixation point offset was observed only when nicotine microinjection was made at the rostral SC (Fig 15B, compared to the result from microinjection at the caudal SC shown in Fig 15A). One of the possibilities that could account for these results is that the fixation-breaking saccades were directly triggered by the visual bursts of rostral SC neurons to the fixation point offset, which would be enhanced by nicotine microinjection. Another possibility is that, because of the tonic activities of rostral SC neurons during active fixation, the basal firing rates of rostral SC neurons seem to be higher than those of caudal SC neurons; accordingly, the firing rates of rostral SC neurons more immediately reach the threshold for triggering saccades than those of caudal SC neurons after nicotine microinjection. In addition to the fixation-breaking saccades, the reaction times of visually guided saccades from the target onset were also decreased by nicotine microinjection at the rostral SC when the targets were presented close to the affected area (Fig 4). These results are consistent with the hypothesis that rostral SC neurons contribute to triggering small contraversive saccades. This hypothesis is also supported by a recent finding that the firing rates of rostral SC

neurons before saccade onset are correlated with the reaction times of small saccades (Krauzlis 2003). These observations do not necessarily exclude the possibility that the tonic activities of rostral SC neurons are involved in active fixation. However, our results are inconsistent with the fixation hypothesis since the reaction times of visually guided saccades passing beyond the affected area were not increased by nicotine microinjection (Fig 4), while the endpoints of the saccades were transiently biased toward the affected area (Fig 7). The fixation hypothesis has been supported by a previous report that artificial manipulation of neuronal activity in the rostral pole of the SC affected generation of saccades (Munoz and Wurtz 1993b). One of the possibilities that could account for the discrepancy between the current and previous reports is the difference of injection sites between the two reports. Bicuculline injection into the rostral pole of the SC inhibited generation of saccades, but small contraversive staircase saccades (< 2 deg in amplitude) were occasionally generated (Munoz and Wurtz 1993b). They suggested that the generation of the small saccades was due to spread of bicuculline into the extrafoveal region of the SC. The injection sites made at the rostral SC in this study seem to correspond to the extrafoveal region in the previous study. Therefore, it might be possible that nicotine microinjection into the rostral pole of the SC, which is the same location as that in the previous report, inhibit generation of saccades. However, in preliminary data analysis, we observed that saccade performance was not modified when nicotine microinjection was made at the more rostro-ventral region that might correspond to the rostral pole of the SC in the previous report, where we encountered neurons showing tonic activities during active fixation (data not shown). This might be explained by a lack of nicotinic receptors on the neurons at the rostral pole of the SC. Nevertheless, this discrepancy should be clarified by a direct comparison between the effects of nicotine and bicuculline microinjections made at the sane region.

Lateral inhibition

The lateral inhibitory interactions in the SC model predict that the reaction times of saccades

toward the targets remote from the affected area should be increased by nicotine microinjection since the activity of neurons at the injection site inhibits the preparatory activities of neurons remote from the injection site (Clark 1999; Findlay and Walker 1999; Godijn and Theeuwes 2002; Munoz and Fecteau 2002; Trappenberg et al. 2001). However, our results are not consistent with this prediction since saccadic reaction times were not increased after microinjection (Figs 3, 4 and 5). Furthermore, an increase in saccadic reaction times was not observed even if the activities of neurons at the injection site were sufficiently enhanced before target onset (Fig 3 and 13). These results are not consistent with pervious reports that local activation or inactivation in the SC affected the reaction times of ipsilateral saccades (Carello and Krauzlis 2003; Schiller et al. 1987). The discrepancy between the results obtained from electrical stimulation (Carello and Krauzlis 2003) versus nicotine microinjection might be explained by activation of axons by electrical stimulation. For example, stimulation of axons from the substantia nigra pars reticulata (SNr) neurons would cause an axonal reflex, which could inhibit neurons remote from the stimulation site. On the other hand, the discrepancy between the results from muscimol injection (Schiller et al. 1987) and current experiments might be explained by the effects on the fixation neurons. If muscimol spreads to the rostral pole of the SC, a decrease in the reaction times of ipsilateral saccades could be accounted for by inactivation of fixation neurons (Munoz and Wurtz 1993b). Based on these considerations, we suggest that the inhibitory interactions in the SC are not strong enough to shape the spatial distribution of neural activity in the SC. Although this concept is in agreement with recent findings (McPeek et al. 2003; McPeek and Keller 2002; Ozen et al. 2004; Port and Wurtz 2003), it appears to be paradoxical if accurate saccades require remote inhibition within the SC map to shape the spatial distribution of ordered presaccadic bursts (but see McPeek and Keller 2002). One of the possible explanations for this discrepancy is that inhibitory control over the SC map is achieved by afferent input from SNr neurons. However, visually guided saccades are quite accurate even when muscimol was locally microinjected into the SNr (Hikosaka and Wurtz 1985b). It is, therefore, possible that inhibitory

intrinsic circuits within the SC can properly shape the presaccadic bursts regardless of whether inhibitory input from the SNr is functional or not. A plausible explanation of these results might be that the strength of inhibitory interactions within the SC depends on the firing rates of SC neurons. The low-frequency preparatory activities of SC neurons might not be strong enough to exert inhibitory effects on the activities of neurons in remote areas. However, the high-frequency presaccadic bursts of SC neurons might be sufficient to drive the inhibitory networks in the SC.

Selection of saccade plans

Local activation and inactivation studies have been carried out in several areas within the brain involved in the control of saccades, such as the FEF (Burman and Bruce 1997; Dias et al. 1995; Dias and Segraves 1999; Schiller and Chou 2000; Sommer and Tehovnik 1997) and SNr (Hikosaka and Wurtz 1985b). Activation of saccade-related areas in the FEF facilitated initiation of saccades toward targets close to the affected area while it inhibited saccades toward targets remote from the affected area (Burman and Bruce 1997; Dias et al. 1995) Inactivation of the SNr facilitated initiation of contralateral saccades while it inhibited ipsilateral saccades (Hikosaka and Wurtz 1985b). Although the effects of inactivation of the FEF on the reaction times of saccades toward targets remote from the affected area were not consistent between studies (Dias and Segraves 1999; Schiller and Chou 2000; Sommer and Tehovnik 1997), it is possible that initiation of saccades might be determined by the distributed circuits interconnecting these areas in a winner-takes-all fashion. The spatial distribution of low-frequency activities in the SC appears to be regulated by inhibitory intrinsic circuits in a push-pull manner (Infante and Leiva 1986). However, it might be merely passive read-out of processes occurring in the neural networks upstream from the SC. This view is supported by a recent report that partial lidocaine inactivation of the paramedian pontine reticular formation, downstream from the SC, inhibited ipsilesional saccades while contralesional saccades were not affected (Barton et al. 2003). The networks upstream from the SC and/or inhibitory input from visually bursting SNr

neurons synapsing with saccade-related SC neurons (Jiang et al. 2003) might explain the inhibitory effect related to the remote distractor effect (Olivier et al. 1999; Walker et al. 1997; Walker et al. 1995; Weber and Fischer 1994). However, it is still unclear whether the visual responses of SC neurons can drive the inhibitory intrinsic circuits in the SC. Further study is required to establish the role of the SC in competitive selection of saccade plans.

References

Aizawa H, Kobayashi Y, Yamamoto M, and Isa T. Injection of nicotine into the superior colliculus facilitates occurrence of express saccades in monkeys. *J Neurophysiol* 82: 1642-1646, 1999.

Arai K, McPeek RM, and Keller EL. Properties of saccadic responses in monkey when multiple competing visual stimuli are present. *J Neurophysiol* 91: 890-900, 2004.

Badler JB and Keller EL. Decoding of a motor command vector from distributed activity in superior colliculus. *Biol Cybern* 86: 179-189, 2002.

Barton EJ, Nelson JS, Gandhi NJ, and Sparks DL. Effects of partial lidocaine inactivation of the paramedian pontine reticular formation on saccades of macaques. *J Neurophysiol* 90: 372-386, 2003.

Beninato M and Spencer RF. A cholinergic projection to the rat superior colliculus demonstrated by retrograde transport of horseradish peroxidase and choline acetyltransferase immunohistochemistry. J Comp Neurol 253: 525-538, 1986.

Burman DD and Bruce CJ. Suppression of task-related saccades by electrical stimulation in the primate's frontal eye field. *J Neurophysiol* 77: 2252-2267, 1997.

Carello CD and Krauzlis RJ. A subtle manipulation of intention: subthreshold microstimulation in the superior colliculus alters saccade and pursuit target choice. *Soc Neurosci Abst* 29: 441.445, 2003.

Clark JJ. Spatial attention and latencies of saccadic eye movements. *Vision Res* 39: 585-602, 1999.

Crist CF, Yamasaki DS, Komatsu H, and Wurtz RH. A grid system and a microsyringe for single cell recording. *J Neurosci Methods* 26: 117-122, 1988.

Dias EC, Kiesau M, and Segraves MA. Acute activation and inactivation of macaque frontal eye field with GABA-related drugs. *J Neurophysiol* 74: 2744-2748, 1995.

Dias EC and Segraves MA. Muscimol-induced inactivation of monkey frontal eye field: effects on visually and memory-guided saccades. *J Neurophysiol* 81: 2191-2214, 1999.

Dorris MC and Munoz DP. A neural correlate for the gap effect on saccadic reaction times in monkey. *J Neurophysiol* 73: 2558-2562, 1995.

Dorris MC and Munoz DP. Saccadic probability influences motor preparation signals and time to saccadic initiation. *J Neurosci* 18: 7015-7026, 1998.

Dorris MC, Pare M, and Munoz DP. Neuronal activity in monkey superior colliculus related to the initiation of saccadic eye movements. *J Neurosci* 17: 8566-8579, 1997.

Doyle M and Walker R. Curved saccade trajectories: voluntary and reflexive saccades curve away from irrelevant distractors. *Exp Brain Res* 139: 333-344, 2001.

Doyle MC and Walker R. Multisensory interactions in saccade target selection: curved saccade trajectories. *Exp Brain Res* 142: 116-130, 2002.

Edelman JA and Keller EL. Dependence on target configuration of express saccade-related activity in the primate superior colliculus. *J Neurophysiol* 80: 1407-1426, 1998.

Everling S, Dorris MC, Klein RM, and Munoz DP. Role of primate superior colliculus in preparation and execution of anti-saccades and pro-saccades. *J Neurosci* 19: 2740-2754, 1999.

Findlay JM and Walker R. A model of saccade generation based on parallel processing and competitive inhibition. *Behav Brain Sci* 22: 661-674; discussion 674-721, 1999.

Fuchs AF and Robinson DA. A method for measuring horizontal and vertical eye movement chronically in the monkey. *J Appl Physiol* 21: 1068-1070, 1966.

Gandhi NJ and Keller EL. Spatial distribution and discharge characteristics of superior colliculus neurons antidromically activated from the omnipause region in monkey. *J Neurophysiol* 78: 2221-2225, 1997.

Glimcher PW and Sparks DL. Effects of low-frequency stimulation of the superior colliculus on spontaneous and visually guided saccades. *J Neurophysiol* 69: 953-964, 1993a.

Glimcher PW and Sparks DL. Representation of averaging saccades in the superior colliculus of the

monkey. *Exp Brain Res* 95: 429-435, 1993b.

Godijn R and Theeuwes J. Programming of endogenous and exogenous saccades: evidence for a competitive integration model. *J Exp Psychol Hum Percept Perform* 28: 1039-1054, 2002.

Gore JL, Everling S, Kobayashi Y, Dorris MC, and Munoz DP. Saccadic preparatory signals in the FEF, SNR and SC. *Soc Neurosci Abst* 464.2, 2002.

Graybiel AM. A stereometric pattern of distribution of acetylthiocholinesterase in the deep layers of the superior colliculus. *Nature* 272: 539-541, 1978.

Green DM and Swets JA. Signal detection theory and psychophysics. *New York: Wiley*, 1966.

Hall WC, Fitzpatrick D, Klatt LL, and Raczkowski D. Cholinergic innervation of the superior colliculus in the cat. J Comp Neurol 287: 495-514, 1989.

Hikosaka O and Wurtz RH. Effects on eye movements of a GABA agonist and antagonist injected into monkey superior colliculus. *Brain Res* 272: 368-372, 1983.

Hikosaka O and Wurtz RH. Modification of saccadic eye movements by GABA-related substances. I. Effect of muscimol and bicuculline in monkey superior colliculus. *J Neurophysiol* 53: 266-291, 1985a.

Hikosaka O and Wurtz RH. Modification of saccadic eye movements by GABA-related substances. II. Effects of muscimol in monkey substantia nigra pars reticulata. *J Neurophysiol* 53: 292-308, 1985b.

Illing RB and Graybiel AM. Convergence of afferents from frontal cortex and substantia nigra onto acetylcholinesterase-rich patches of the cat's superior colliculus. Neuroscience 14: 455-482, 1985.

Infante C and Leiva J. Simultaneous unitary neuronal activity in both superior colliculi and its relation to eye movements in the cat. *Brain Res* 381: 390-392, 1986.

Isa T, Endo T, and Saito Y. Nicotinic facilitation of signal transmission in the local circuits of the rat superior colliculus. *Soc Neurosci Abst* 60: 13, 1998.

Jiang H, Stein BE, and McHaffie JG. Opposing basal ganglia processes shape midbrain visuomotor activity bilaterally. *Nature* 424: 982-986, 2003.

Kobayashi Y, Inoue Y, Yamamoto M, Isa T, and Aizawa H. Contribution of pedunculopontine tegmental nucleus neurons to performance of visually guided saccade tasks in monkeys. *J Neurophysiol* 88: 715-731, 2002.

Krauzlis RJ. Neuronal activity in the rostral superior colliculus related to the initiation of pursuit and saccadic eye movements. *J Neurosci* 23: 4333-4344, 2003.

Krauzlis RJ, Basso MA, and Wurtz RH. Shared motor error for multiple eye movements. *Science* 276: 1693-1695, 1997.

Krauzlis RJ, Basso MA, and Wurtz RH. Discharge properties of neurons in the rostral superior colliculus of the monkey during smooth-pursuit eye movements. *J Neurophysiol* 84: 876-891, 2000.

Lebedev S, Van Gelder P, and Tsui WH. Square-root relations between main saccadic parameters. *Invest Ophthalmol Vis Sci* 37: 2750-2758, 1996.

Lee C, Rohrer WH, and Sparks DL. Population coding of saccadic eye movements by neurons in the superior colliculus. *Nature* 332: 357-360, 1988.

Li F, Endo T, Isa T. Presynaptic muscarinic acetylcholine receptors suppress GABAergic synaptic transmission in the intermediate gray layers of mouse superior colliculus. *Eur J Neurosci,* in press.

Liston DB and Krauzlis RJ. Saccade trigger signal encoded as firing rate difference in superior colliculus. *Soc Neurosci Abst* 29: 187.186, 2003.

Ma TP, Graybiel AM, and Wurtz RH. Location of saccade-related neurons in the macaque superior colliculus. *Exp Brain Res* 85: 21-35, 1991.

McIlwain JT. Lateral spread of neural excitation during microstimulation in intermediate gray layer of cat's superior colliculus. *J Neurophysiol* 47: 167-178, 1982.

McPeek RM, Han JH, and Keller EL. Competition between saccade goals in the superior colliculus produces saccade curvature. *J Neurophysiol* 89: 2577-2590, 2003.

McPeek RM and Keller EL. Short-term priming, concurrent processing, and saccade curvature during a target selection task in the monkey. *Vision Res* 41: 785-800, 2001.

McPeek RM and Keller EL. Superior colliculus activity related to concurrent processing of saccade goals in a visual search task. *J Neurophysiol* 87: 1805-1815, 2002.

Meredith MA and Ramoa AS. Intrinsic circuitry of the superior colliculus: pharmacophysiological identification of horizontally oriented inhibitory interneurons. *J Neurophysiol* 79: 1597-1602, 1998.

Moschovakis AK, Karabelas AB, and Highstein SM. Structure-function relationships in the primate superior colliculus. II. Morphological identity of presaccadic neurons. *J Neurophysiol* 60: 263-302, 1988.

Munoz DP and Fecteau JH. Vying for dominance: dynamic interactions control visual fixation and saccadic initiation in the superior colliculus. *Prog Brain Res* 140: 3-19, 2002.

Munoz DP and Istvan PJ. Lateral inhibitory interactions in the intermediate layers of the monkey superior colliculus. *J Neurophysiol* 79: 1193-1209, 1998.

Munoz DP and Wurtz RH. Fixation cells in monkey superior colliculus. I. Characteristics of cell discharge. *J Neurophysiol* 70: 559-575, 1993a.

Munoz DP and Wurtz RH. Fixation cells in monkey superior colliculus. II. Reversible activation and deactivation. *J Neurophysiol* 70: 576-589, 1993b.

Olivier E, Dorris MC, and Munoz DP. Lateral interactions in the superior colliculus, not an extended fixation zone, can account for the remote distractor effect. *Behav Brain Sci* 22: 694-695, 1999.

Ottes FP, Van Gisbergen JA, and Eggermont JJ. Visuomotor fields of the superior colliculus: a quantitative model. *Vision Res* 26: 857-873, 1986.

Ozen G, Helms MC, and Hall WC. Intracollicular neuronal network. In: *The superior colliculus*, edited by Hall WC and Moschovakis AK. Boca Raton, FL: CRC Press, 2004, p. 147-158.

Pare M. Ballistic movement processing: saccade initiation is linked to an invariant trigger threshold in superior colliculus. *Soc Neurosci Abst* 29: 79.17, 2003.

Pare M and Hanes DP. Controlled movement processing: superior colliculus activity associated with countermanded saccades. *J Neurosci* 23: 6480-6489, 2003.

Pettit DL, Helms MC, Lee P, Augustine GJ, and Hall WC. Local excitatory circuits in the intermediate gray layer of the superior colliculus. *J Neurophysiol* 81: 1424-1427, 1999.

Port NL and Wurtz RH. Sequential activity of simultaneously recorded neurons in the superior colliculus during curved saccades. *J Neurophysiol* 90: 1887-1903, 2003.

Quaia C, Aizawa H, Optican LM, and Wurtz RH. Reversible inactivation of monkey superior colliculus. II. Maps of saccadic deficits. *J Neurophysiol* 79: 2097-2110, 1998.

Robinson DA. Eye movements evoked by collicular stimulation in the alert monkey. *Vision Res* 12: 1795-1808, 1972.

Saito Y and Isa T. Local excitatory network and NMDA receptor activation generate a synchronous and bursting command from the superior colliculus. *J Neurosci* 23: 5854-5864, 2003.

Saslow MG. Effects of components of displacement-step stimuli upon latency for saccadic eye movement. *J Opt Soc Am* 57: 1024-1029, 1967.

Schiller PH and Chou I. The effects of anterior arcuate and dorsomedial frontal cortex lesions on visually guided eye movements in the rhesus monkey: 1. Single and sequential targets. *Vision Res* 40: 1609-1626, 2000.

Schiller PH, Sandell JH, and Maunsell JH. The effect of frontal eye field and superior colliculus lesions on saccadic latencies in the rhesus monkey. *J Neurophysiol* 57: 1033-1049, 1987.

Schiller PH and Stryker M. Single-unit recording and stimulation in superior colliculus of the alert rhesus monkey. *J Neurophysiol* 35: 915-924, 1972.

Sommer MA and Tehovnik EJ. Reversible inactivation of macaque frontal eye field. *Exp Brain Res* 116: 229-249, 1997.

Sparks D, Rohrer WH, and Zhang Y. The role of the superior colliculus in saccade initiation: a study of express saccades and the gap effect. *Vision Res* 40: 2763-2777, 2000.

Sparks DL and Hartwich-Young R. The deep layers of the superior colliculus. *Rev Oculomot Res* 3: 213-255, 1989.

Stanford TR. Signal coding in the primate superior colliculus revealed through the use of artificial signals. In: *The superior colliculus*, edited by Hall WC and Moschovakis AK. Boca Raton, FL: CRC Press, 2004, p. 35-53.

Trappenberg TP, Dorris MC, Munoz DP, and Klein RM. A model of saccade initiation based on the competitive integration of exogenous and endogenous signals in the superior colliculus. *J Cogn Neurosci* 13: 256-271, 2001.

Uka T and DeAngelis GC. Contribution of area MT to stereoscopic depth perception: choice-related response modulations reflect task strategy. *Neuron* 42: 297-310, 2004.

van Opstal AJ and van Gisbergen JA. Role of monkey superior colliculus in saccade averaging. *Exp Brain Res* 79: 143-149, 1990.

Walker R, Deubel H, Schneider WX, and Findlay JM. Effect of remote distractors on saccade programming: evidence for an extended fixation zone. *J Neurophysiol* 78: 1108-1119, 1997.

Walker R, Kentridge RW, and Findlay JM. Independent contributions of the orienting of attention, fixation offset and bilateral stimulation on human saccadic latencies. *Exp Brain Res* 103: 294-310, 1995.

Weber H and Fischer B. Differential effects of non-target stimuli on the occurrence of express saccades in man. *Vision Res* 34: 1883-1891, 1994.

Figure legends

Figure 1: Endpoints of spontaneous saccades (N15-1). A, B and C: “baseline” (15-minute period before microinjection), “injection” (15-mintute period after microinjection) and “recovery” (15-minute period following the time-window of the “injection” data) data, respectively. The initial points of the saccade were aligned to the origin of the coordinate axes. Gray crosses indicate the center of the affected area.

Figure 2: Summary of effects on endpoints of spontaneous saccades. Circles, triangles and stars indicate data from monkey M, D and H, respectively. Filled and open symbols indicate data in which statistical significances were observed (U-test $p < 0.05$ with Bonferroni correction). Dotted lines indicate equality lines.

Figure 3: Reaction times of visually guided saccades (N15-1). Inset: the arrangement of targets. Gray cross indicates the center of the affected area. Black cross indicates the fixation point. A and B: time-courses of changes in reaction times. A and B show data for the targets labeled as A and B in the inset. Horizontal black bars indicate the period of nicotine microinjection. C: mean reaction times against the directions of targets. Data for the gap and overlap tasks were pooled together. The time-windows for the “baseline” and “injection” data included the 15-minute period immediately prior to and following the start of nicotine microinjection, respectively. Dotted line indicates the direction of the center of the affected area. Error bars indicate standard error.

Figure 4: Effects of nicotine microinjection into rostral SC on reaction times of visually guided saccades (N5-1). A and B: time-course of changes in the reaction times of saccades toward the targets labeled as A (open circles) and B (open triangles) in the inset, respectively. C: mean reaction times against target eccentricities. The time-windows for the “baseline” and “injection” data were included

the 15-minute period immediately before and after the start of the nicotine microinjection, respectively. Dotted line indicates the amplitude of the center of the affected area.

Figure 5: Summary of effects on reaction times of visually guided saccades. Gray crosses indicate the normalized target points. Each data point indicates the position of the injection site relative to the normalized target point. The numbers on the left and bottom of the panel A indicate the directions and amplitudes of saccades encoded by the injection sites relative to the normalized target point, respectively. A: decrease in reaction times (U-test $p < 0.05$ with Bonferroni correction). B: increase in reaction times (U-test $p < 0.05$ with Bonferroni correction). C: no change in reaction times (U-test $p > 0.05$ with Bonferroni correction). Circles and triangles indicate data from monkey M and D, respectively.

Figure 6: Endpoints of visually guided saccades (N15-1). A and B: trajectories before and after microinjection, respectively. Two consecutive saccades are shown. C and D: time-course of changes in the distances of endpoints from the center of the affected area for the data labeled as C and D in A. E: mean endpoints before (open circles) and after microinjection (diamonds). Black, gray and open diamonds indicate U-test $p < 0.005$, $p < 0.05$ and $p > 0.05$, respectively. These saccade endpoints were calculated after the initial points of the saccades were aligned to the origin of the coordinate axes. The time-windows for the data before and after microinjection included the 15-minute period immediately before and after the start of microinjection, respectively. Error bars indicating standard errors are not shown since they are smaller than the markers.

Figure 7: Effects of nicotine microinjection into rostral SC on amplitudes of visually guided saccades (N5-1). A and B: time-course of changes in the amplitudes of saccades toward the targets labeled as A (open circles) and B (open triangles) in the inset. C: mean saccade amplitudes against target

eccentricities. The “baseline” and “injection” data were recorded during the 15-minute period immediately before and after the start of injection, respectively. Dotted line indicates the amplitude of the center of the affected area.

Figure 8: Summary of effects on endpoints of visually guided saccades. A: bias of endpoints toward the affected area (U-test $p < 0.05$ with Bonferroni correction). B: bias of endpoints away from the affected area (U-test $p < 0.05$ with Bonferroni correction). C: no change in endpoints (U-test $p > 0.05$ with Bonferroni correction). Circles and triangles indicate the data from monkey M and D, respectively.

Figure 9: Curved trajectories of visually guided saccades (N22-1). A: the trajectories of saccades from the "baseline" (blue line) and "injection" (red line) data are superimposed. The “baseline” and “injection” data were recorded during the 15-minute period immediately before and after microinjection, respectively. B: time-course of changes in the curvature indices of the saccades. The curvature indices were normalized by those before the microinjection. Some saccades whose endpoints were biased toward the affected area were excluded from the current analysis (see Methods), leading to the lack of data points between 3 to 7 minutes after the start of microinjection.

Figure 10: Summary of effects on trajectories of visually guided saccades. A: curved trajectories toward the affected area (U-test $p < 0.05$ with Bonferroni correction). B: curved trajectories away from the affected area (U-test $p < 0.05$ with Bonferroni correction). Circles and triangles indicate data from monkey M and D, respectively.

Figure 11: Task dependent effects of nicotine microinjection on reaction times of visually guided saccades (N19-1). In this experiment, targets were symmetrically presented in 8 directions as in the

case of the inset in Figure 2. The data were derived from a target (eccentricity 24.1 deg, direction 54.0°) presented close to the affected area (amplitude 24.0 deg, direction 54.4°). A: time-course of changes in reaction times. B: ROC curves for each task. The ROC curves were calculated from the distribution of the pre- and post microinjection reaction times for each task. The dotted and continuous lines indicate the data for the gap and step tasks, respectively. The time-windows for the data after microinjection ranged from 0 to 30 min (black lines) or from 30 to 60 min (red lines).

Figure 12: Summary of task dependent effects on reaction time of visually guided saccades. An ROC area below 0.5 indicates that reaction times were decreased after nicotine exposure. The abscissa and ordinate indicate ROC area for the gap and no-gap tasks, respectively. Circles and triangles indicate data from monkey M and D, respectively. Filled and open symbols indicate data in which reaction times were reduced in both or either task, respectively (Permutation test $p < 0.05$ with Bonferroni correction). Dotted line indicates equality line. The time-windows for the "baseline" and "injection" data included a 30-minute period immediately before and after the start of microinjection.

Figure 13: Fixation-breaking saccades initiated within 80 ms from target onset (N15-1). A and B: saccade trajectories obtained during 15-minute period before and after microinjection, respectively. C: time-courses of changes in the distances of saccade endpoints from the center of the affected area.

Figure 14: Summaries of task dependent effects on fixation-breaking saccades. A: comparison between the effects on the frequencies of fixation-breaking saccades in the gap and no-gap tasks. The "Δerror rate" indicates a difference between the proportions of trials in which fixation-breaking saccades were generated before and after microinjection. The Δerror rate becomes positive if fixation-breaking saccades were facilitated by microinjection. B: comparison of saccade endpoints between the tasks. Circles and triangles indicate data from monkey M and D, respectively. Filled and

open symbols indicate data in which statistical significances were observed (U-test $p < 0.05$ with Bonferroni correction).

Figure 15: Reaction times of fixation-breaking saccades from fixation point offset in gap task. A and B: time-course of changes in the reaction times of fixation-breaking saccades from the fixation point offset when nicotine microinjection was made at the caudal (N15-1) or rostral (N5-1) region, respectively. Dotted lines indicate the timing of target onset.

Figure 16: Effects of vehicle (PBS) microinjection into caudal SC on reaction times of visually guided saccades (P2-1). A: time-course of changes in the reaction times of saccades toward the targets labeled as A in the inset. B: mean reaction times against the directions of targets. The time-windows for the “baseline” and “injection” data included the 15-minute period immediately prior to and following the start of nicotine microinjection, respectively.

Table 1. Summary of injections

Experiment Number	Monkey	Saccade		Injection	
		Amplitude (deg)	Direction (deg)	Concentration (mM)	Volume (μl)
N1-1	M	1.7	65	10	0.4
N2-1	H	1.8	11	100	1
N3-1	M	1.8	359	10	1
N4-1	M	1.9	127	10	0.4
N5-1	M	2.4	5	10	1
N6-1	H	2.9	29	50	1
N6-2	H	2.9	29	50	1
N7-1	M	6.6	304	50	1
N7-2	M	6.6	304	50	1
N8-1	M	6.9	148	10	0.4
N8-2	M	6.9	148	10	0.2
N9-1	M	8.2	157	10	0.6
N9-2	M	8.2	157	10	0.4
N10-1	M	8.9	133	10	1
N10-2	M	8.9	133	10	1
N11-1	M	8.9	133	10	1
N11-2	M	8.9	133	10	1
N12-1	M	11	82	10	1
N13-1	D	11.2	88	100	0.6
N13-2	D	11.2	88	100	0.6
N13-3	D	11.2	88	100	0.6
N14-1	M	12.3	95	10	1
N15-1	D	13.1	48	100	0.6
N15-2	D	13.1	48	100	0.6
N15-3	D	13.1	48	100	0.2
N15-4	D	13.1	48	100	0.2
N16-1	D	13.1	356	50	0.6
N17-1	M	13.2	93	10	0.8
N18-1	M	17.6	49	10	1
N18-2	M	17.6	49	10	1
N19-1	M	24	54	10	1
N19-2	M	24	54	10	1
N20-1	M	24	54	50	1
N21-1	D	25.1	12	100	0.6
N22-1	D	29.2	155	100	0.6
N22-2	D	29.2	155	100	0.4
N22-3	D	29.2	155	100	0.6
P1-1	M	6.9	72	0	1
P1-2	M	6.9	72	0	1
P2-1	M	8.9	133	0	1
P2-2	M	8.9	133	0	1
P3-1	D	29.2	155	0	1
P3-2	D	29.2	155	0	1

"N" and "P" indicate nicotine and PBS, respectively. Injections with the same first numbers and different second numbers correspond to sequential injections.

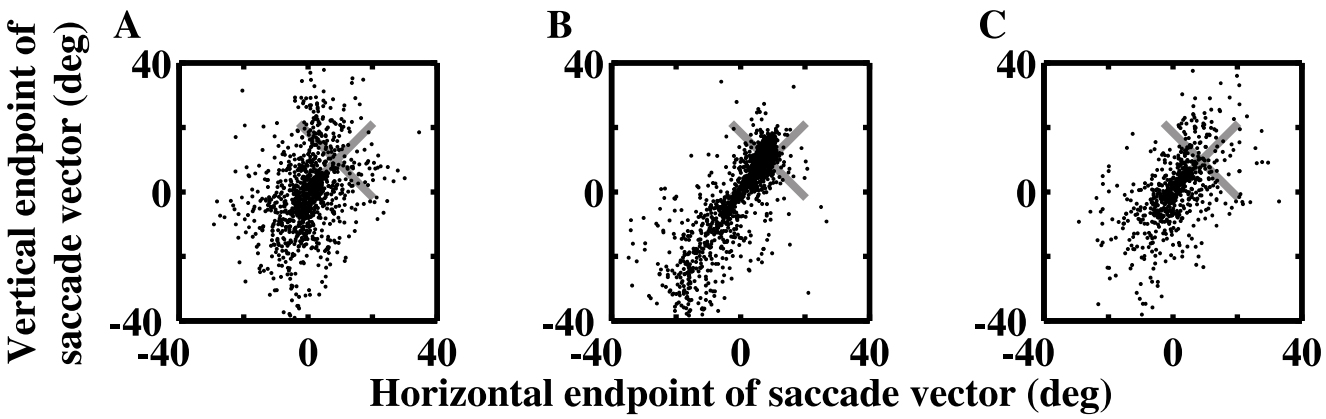
A
B
C
Vertical endpoint of saccade vector (deg)
40
0
-40
-40
0
40
Horizontal endpoint of saccade vector (deg)

Figure 1

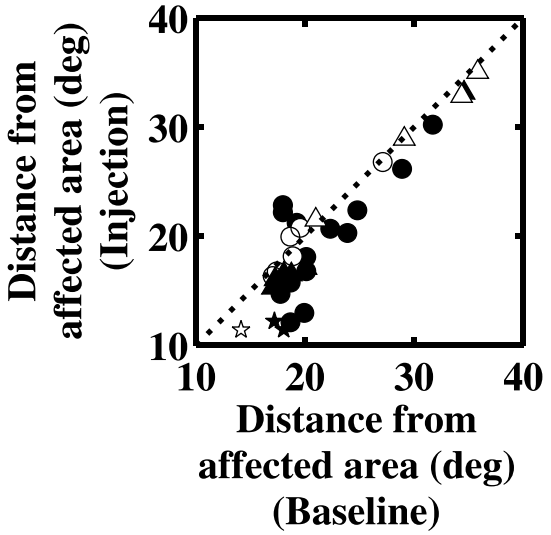
Distance from affected area (deg) (Injection)
40
30
20
10
10
20
30
40
Distance from affected area (deg) (Baseline)

Figure 2

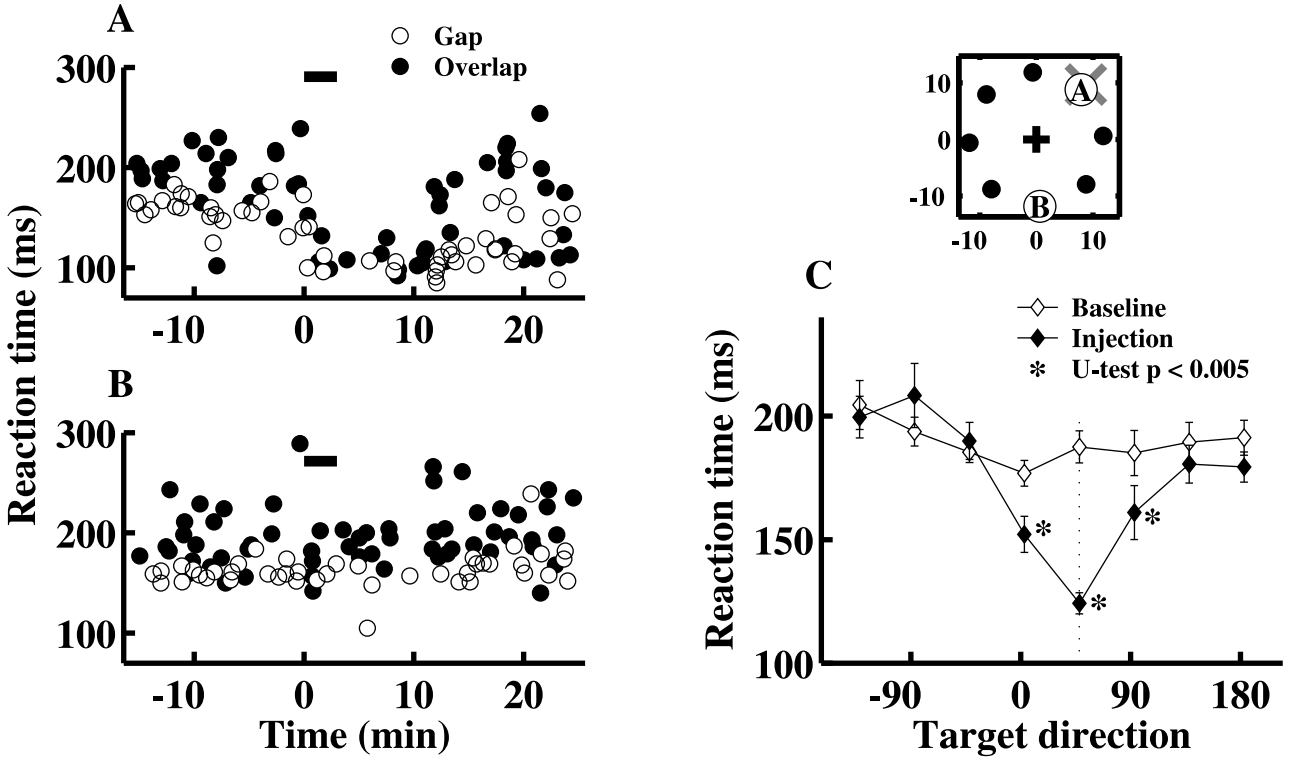
A
Gap
Overlap
300
200
100
-10
0
10
20
B
300
200
100
-10
0
10
20
Reaction time (ms)
Time (min)
10
0
-10
A
B
-10
0
10
C
Baseline
Injection
* U-test p < 0.005
200
150
100
-90
0
90
180
Reaction time (ms)
Target direction

Figure 3

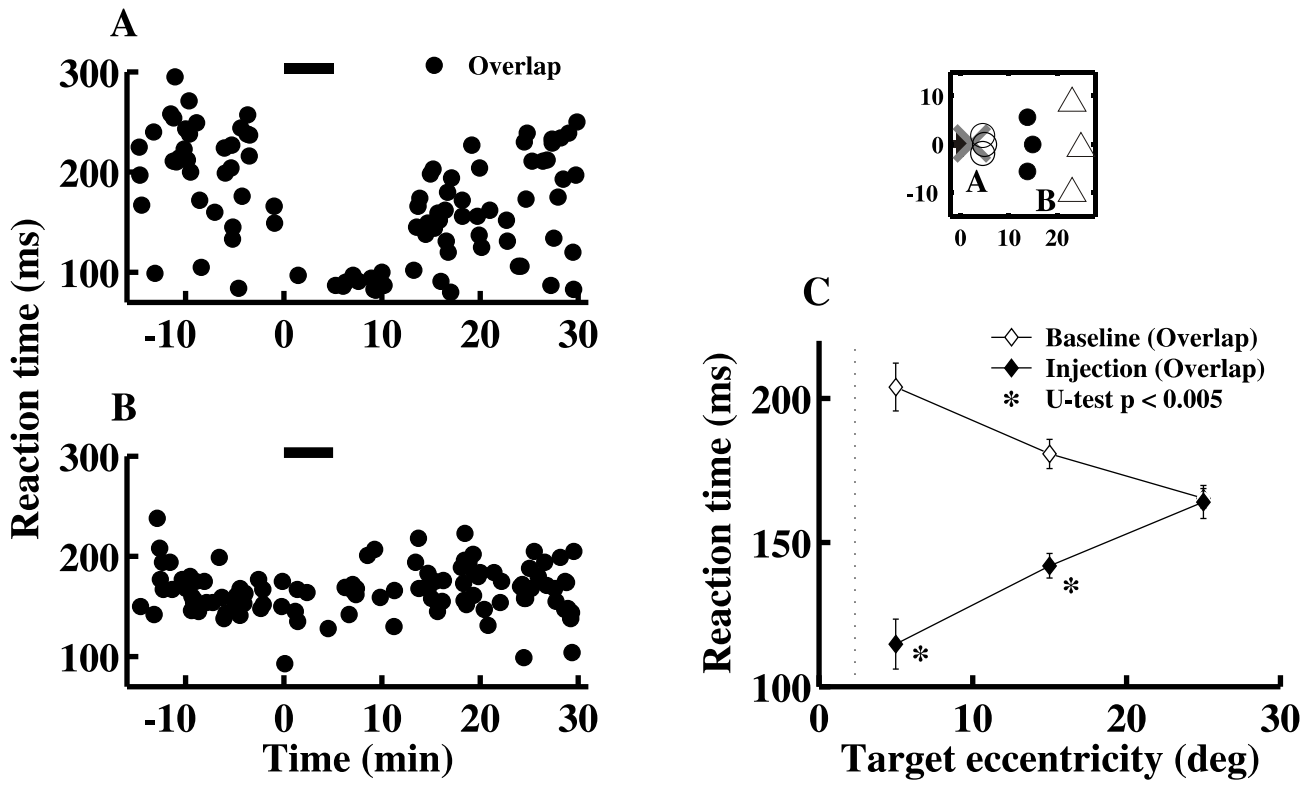
A
Overlap
300
200
100
-10
0
10
20
30
B
Reaction time (ms)
Time (min)
10
0
-10
A
B
0
10
20
C
Baseline (Overlap)
Injection (Overlap)
U-test p < 0.005
Reaction time (ms)
200
150
100
Target eccentricity (deg)

Figure 4

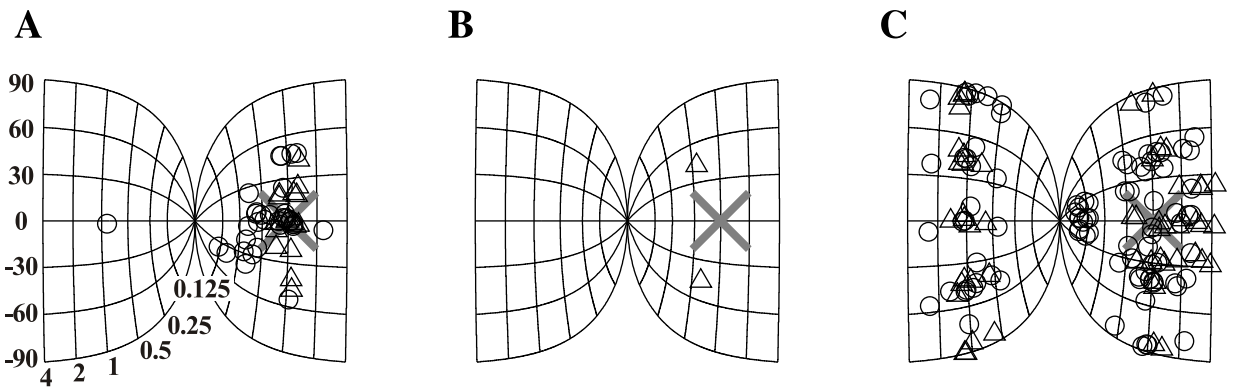

Figure 5

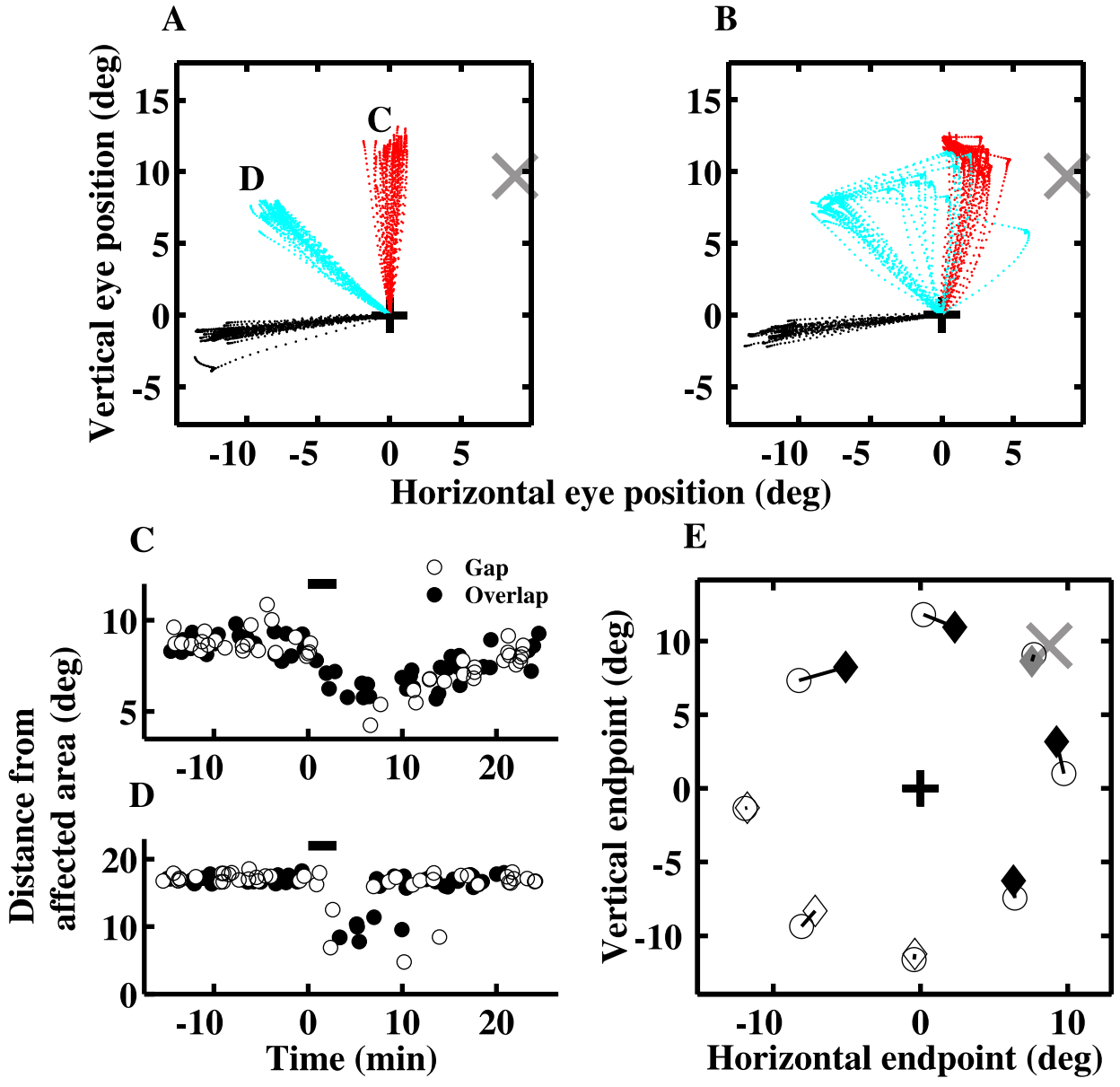
A
B
C
D
Vertical eye position (deg)
Horizontal eye position (deg)
C
D
Gap
Overlap
Distance from affected area (deg)
Time (min)
E
Vertical endpoint (deg)
Horizontal endpoint (deg)

Figure 6

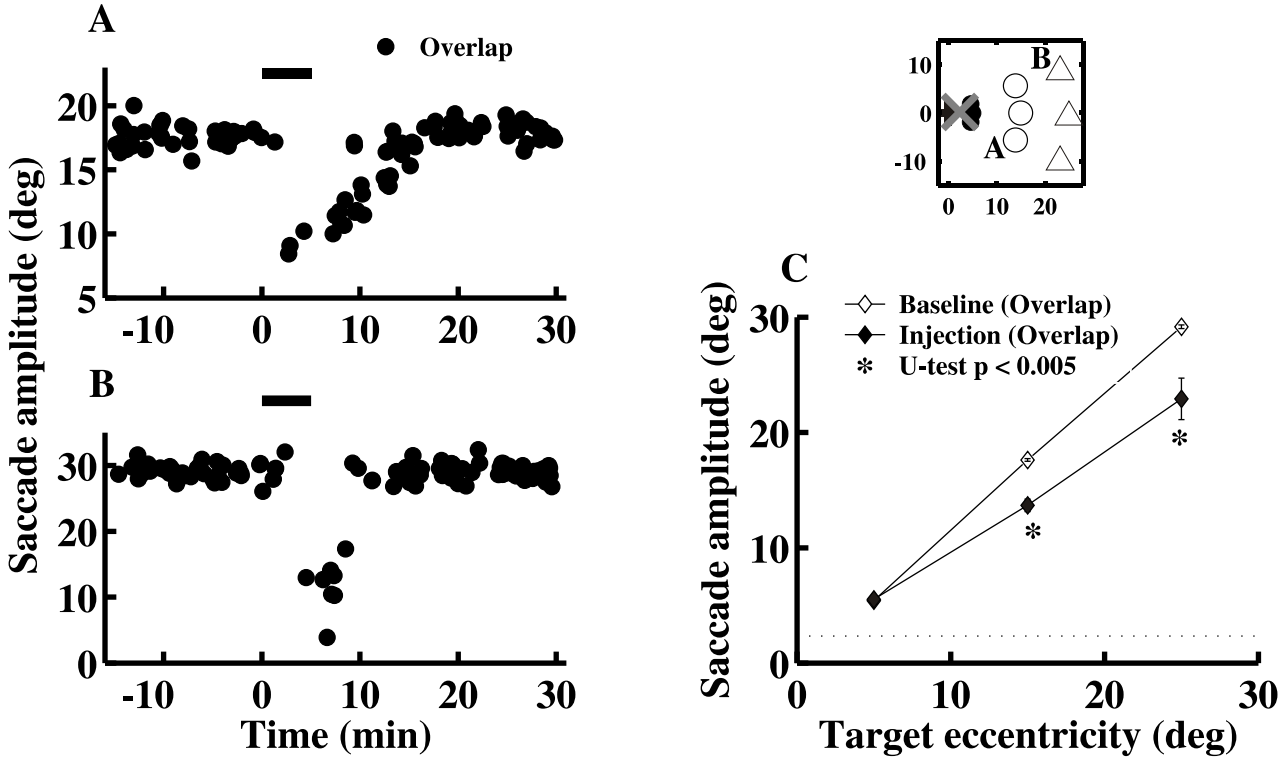
A
Overlap
20
15
10
5
-10
0
10
20
30
B
30
20
10
0
-10
0
10
20
30
Saccade amplitude (deg)
Time (min)
10
0
-10
B
A
0
10
20
C
Baseline (Overlap)
Injection (Overlap)
U-test p < 0.005
30
20
10
0
0
10
20
30
Saccade amplitude (deg)
Target eccentricity (deg)

Figure 7

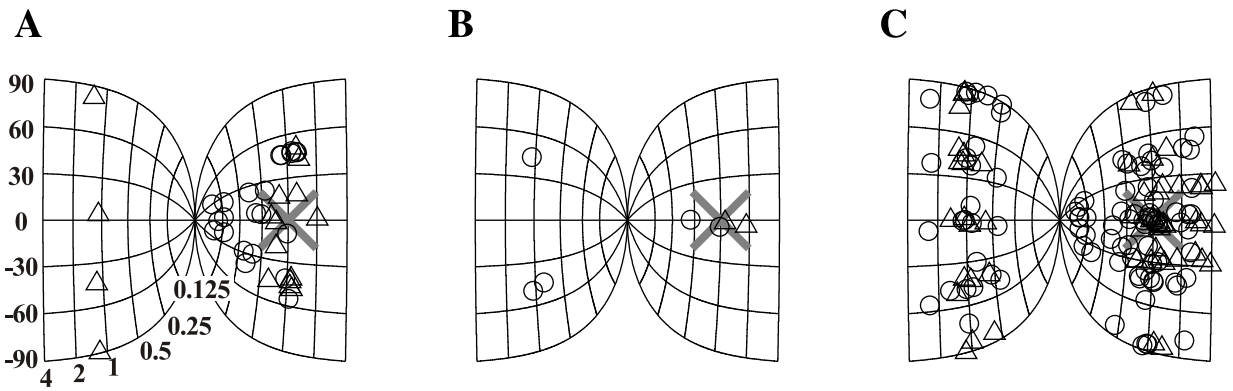

Figure 8

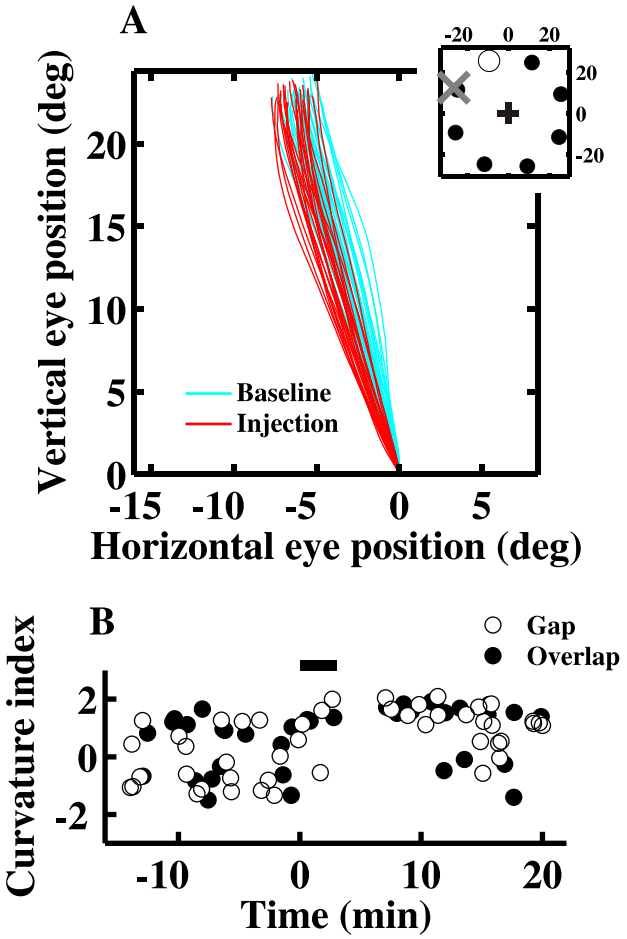
A
-20
0
20
20
0
-20
Vertical eye position (deg)
20
15
10
5
0
Baseline
Injection
-15
-10
-5
0
5
Horizontal eye position (deg)
B
Gap
Overlap
Curvature index
2
0
-2
-10
0
10
20
Time (min)

Figure 9

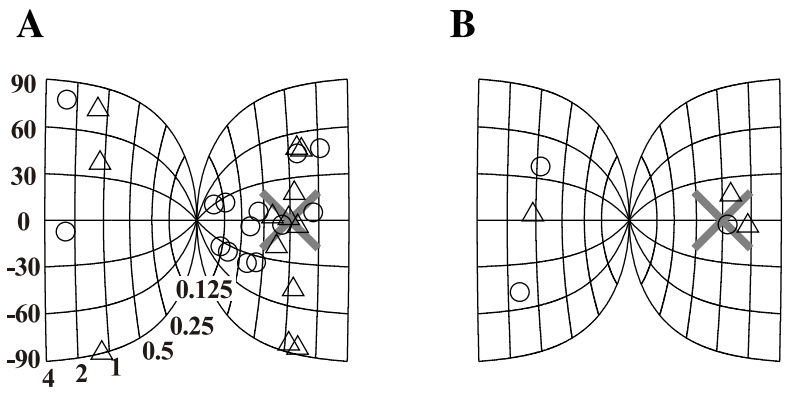

Figure 10

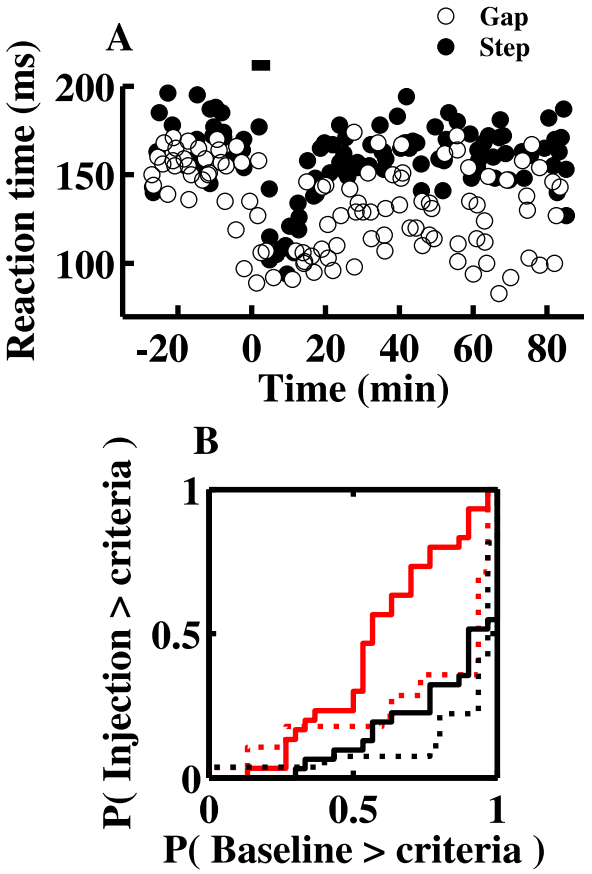
A
Gap
Step
Reaction time (ms)
200
150
100
-20
0
20
40
60
80
Time (min)
B
P(Injection > criteria)
1
0.5
0
0
0.5
1
P(Baseline > criteria)

Figure 11

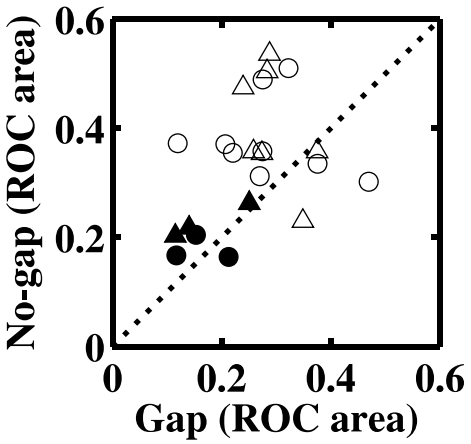

Figure 12

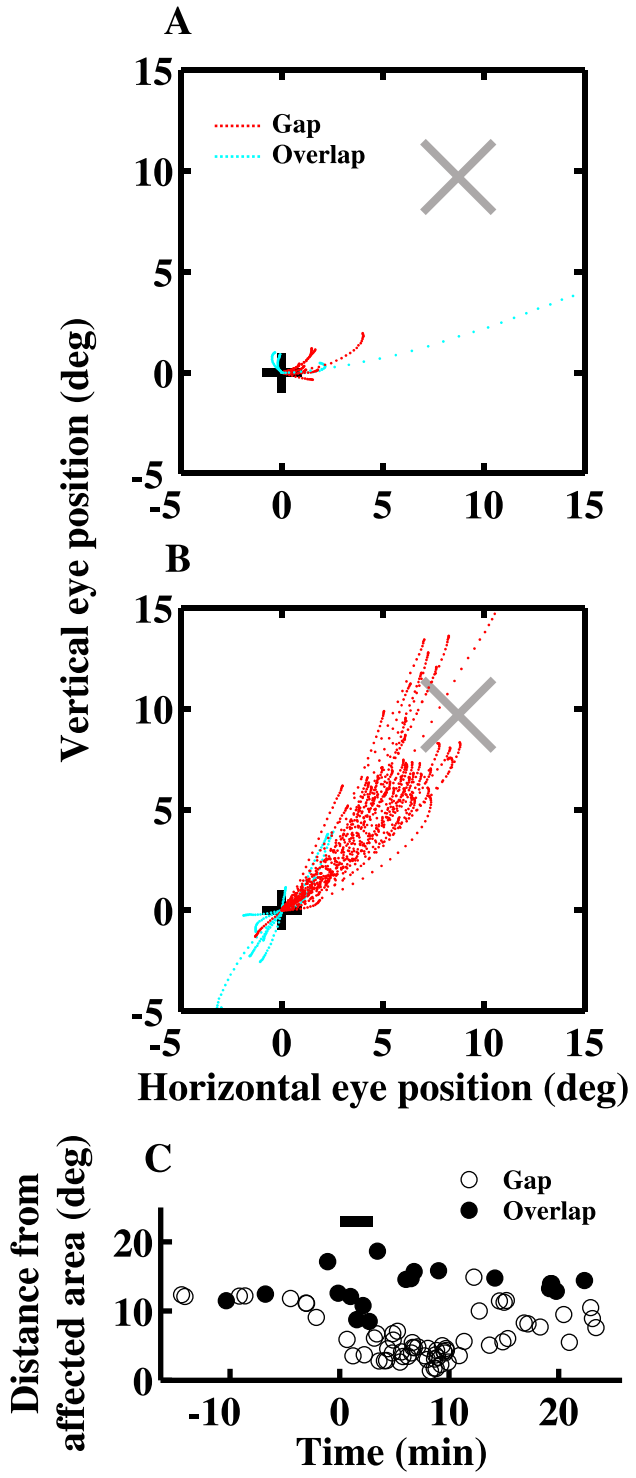
A
B
C
Gap
Overlap
Vertical eye position (deg)
Horizontal eye position (deg)
Distance from affected area (deg)
Time (min)
15
10
5
0
-5
-10
20

Figure 13

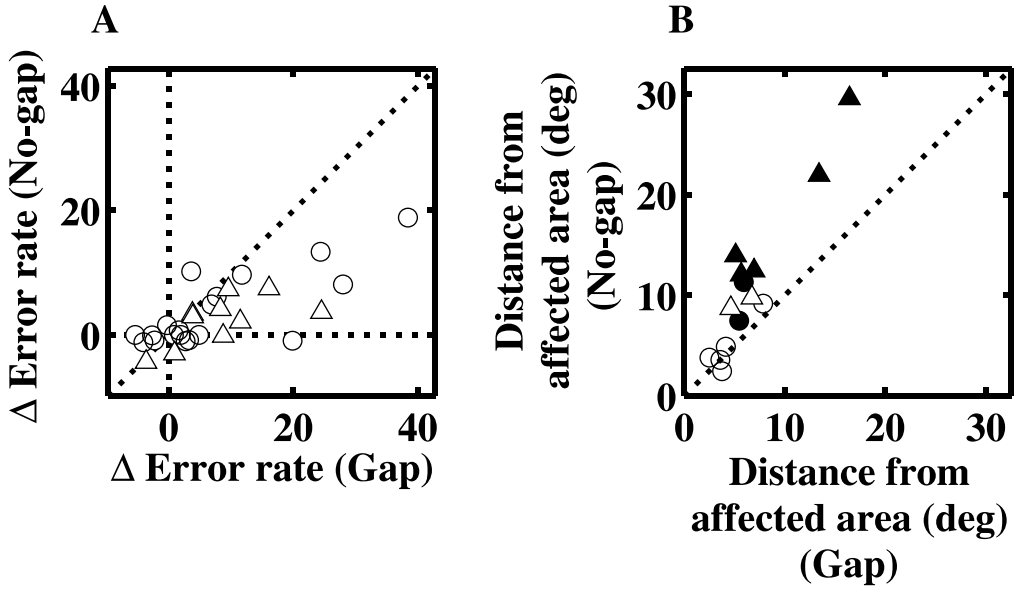
A
Δ Error rate (No-gap)
40
20
0
0
20
40
Δ Error rate (Gap)
B
Distance from affected area (deg) (No-gap)
30
20
10
0
0
10
20
30
Distance from affected area (deg) (Gap)

Figure 14

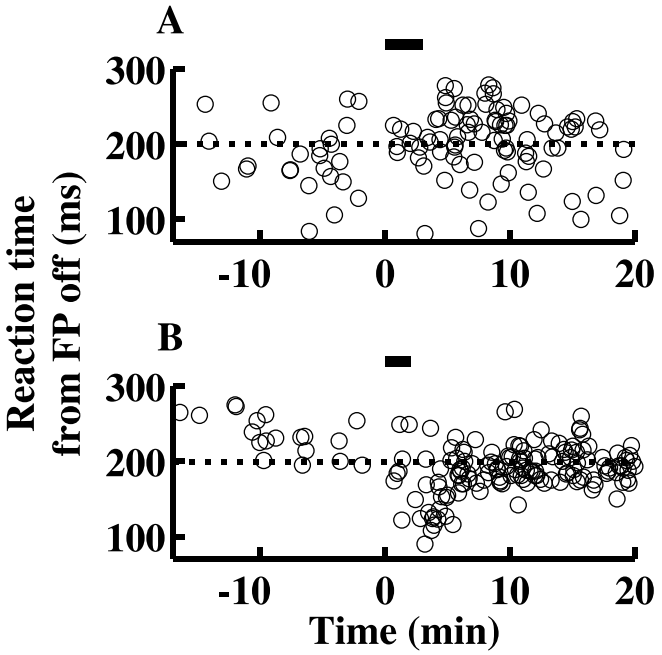
A
300
200
100
-10
0
10
20
B
300
200
100
-10
0
10
20
Reaction time
from FP off (ms)
Time (min)

Figure 15

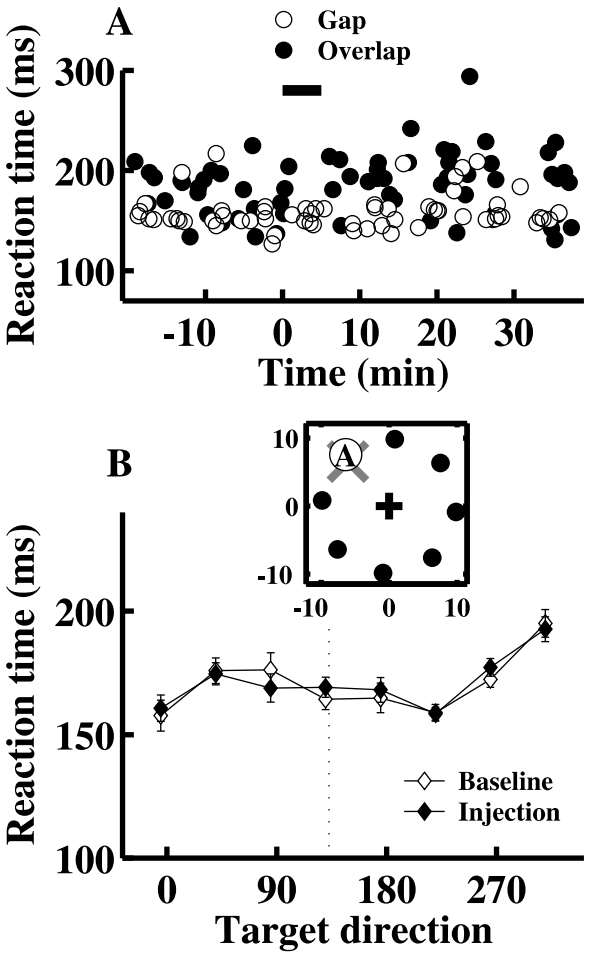
A
Gap
Overlap
Reaction time (ms)
300
200
100
-10
0
10
20
30
Time (min)
B
10
0
-10
-10
0
10
A
Reaction time (ms)
200
150
100
Baseline
Injection
0
90
180
270
Target direction

Figure 16